

1 **Tracking Rodinia into the Neoproterozoic: new
2 paleomagnetic constraints from the Jacobsville
3 Formation**

4 **Yiming Zhang¹, Eben B. Hodgin^{1,2}, Tadesse Alemu¹, James Pierce^{1,3},
5 Anthony Fuentes¹, Nicholas L. Swanson-Hysell¹**

6 ¹Department of Earth and Planetary Science, University of California, Berkeley, CA, USA

7 ²Department of Earth, Environmental, and Planetary Science, Brown University, Providence, RI, USA

8 ³Department of Earth and Planetary Sciences, Yale University, CT, USA

9 **Key Points:**

- 10 • Siltstones and fine-grained sandstones of the ca. 990 Ma Jacobsville Formation
11 have primary magnetization held by detrital hematite.
- 12 • Following closure of the Unimos Ocean and onset of the Grenvillian orogeny in the
13 late Mesoproterozoic, Laurentia's motion went from fast to slow.
- 14 • The pole position and age suggests that the paleomagnetic poles of the Grenville
15 Loop are younger than in previous interpretations.

Corresponding author: Yiming Zhang, yimingzhang@berkeley.edu

Abstract

The paleogeography of Laurentia throughout the Neoproterozoic is critical for reconstructing global paleogeography due to its central position in the supercontinent Rodinia. We develop a new paleomagnetic pole from red siltstones and fine-grained sandstones of the early Neoproterozoic Jacobsville Formation which is now constrained to be ca. 990 Ma in age. High-resolution thermal demagnetization experiments resolve detrital remanent magnetizations held by hematite. These directions were reoriented within siltstone intraclasts and pass intraformational conglomerate tests—giving confidence that the magnetization is detrital and primary. An inclination-corrected mean paleomagnetic pole position for the Jacobsville Formation indicates that Laurentia’s motion slowed down significantly following the onset of the Grenvillian orogeny. Prior rapid plate motion associated with closure of the Unimos Ocean between 1110 and 1090 Ma transitioned to slow drift of Laurentia across the equator in the late Mesoproterozoic to early Neoproterozoic. We interpret the distinct position of this well-dated pole from those in the Grenville orogen that have been assigned a similar age to indicate that the ages of the poles associated with the Grenville Loop likely need to be revised to be younger due to prolonged exhumation.

Plain Language Summary

There have been times in Earth history when many of the continents are joined together into a big continent that is called a supercontinent. The most recent supercontinent is Pangea which had Africa at its center. An older supercontinent called Rodinia formed about 1 billion years ago and had North America at its center. The old parts of North America that were in the supercontinent are called Laurentia. The position of Laurentia is key to understanding where Rodinia was and how different continents were connected in the supercontinent. We now know the age of sedimentary rocks called the Jacobsville Formation that were deposited in ancient rivers and can use these rocks to determine the past position of Laurentia (and therefore Rodinia) 990 million years ago using paleomagnetism. This position is quite different in current interpretations which rely on data from rocks that cooled slowly within an ancient mountain belt that formed when the supercontinent assembled—they likely show where the supercontinent was after 990 Ma. As a result, we have a new understanding of where the supercontinent was that can enable further progress in putting all the pieces together to further understand the ancient Earth.

Introduction

The extensively studied paleomagnetic records of ca. 1109 to 1084 Ma volcanics and intrusions associated with the North American Midcontinent Rift provide crucial constraints on the paleogeography of Laurentia in the late Mesoproterozoic Era (Halls & Pesonen, 1982; Fairchild et al., 2017; Swanson-Hysell, Ramezani, et al., 2019). The resulting sequence of poles known as the Keweenawan Track is a central record for reconstructing the assembly of the ancient supercontinent Rodinia (Evans, 2021). An advantage of intracratonic magmatic events, such as those preserved in the Midcontinent Rift, is that they lead to emplacement of igneous rocks that can readily retain primary thermal remanent magnetization (TRM) that can be confidently associated with the emplacement age of the unit. However, following the development of the Midcontinent Rift, there was a ~300 Myr quiescence in known intracratonic magmatic activity in Laurentia that lasted until the emplacement of the ca. 775 Ma Gunbarrel large igneous province (Harlan et al., 2003; Mackinder et al., 2019; Swanson-Hysell, 2021). The lack of Laurentian rocks with primary TRM in the early Neoproterozoic has led paleogeographic reconstructions to be reliant on magnetizations acquired by rocks that were metamorphosed during the ca. 1090 to 980 Ma Grenvillian orogeny (Rivers, 2008; Rivers et al., 2012; Swanson-

66 Hysell et al., 2023). However, rocks within the orogen acquired their magnetizations during
 67 exhumation after peak metamorphic conditions (McWilliams & Dunlop, 1975). As
 68 a result, the timing of remanence acquisition needs to be constrained through the more
 69 difficult task of dating cooling associated with exhumation. This gap in well-dated paleo-
 70 magnetic poles for Laurentia in the late Mesoproterozoic to mid-Neoproterozoic contributes
 71 to uncertainty in paleogeography at that time including the configuration of the
 72 supercontinent Rodinia.

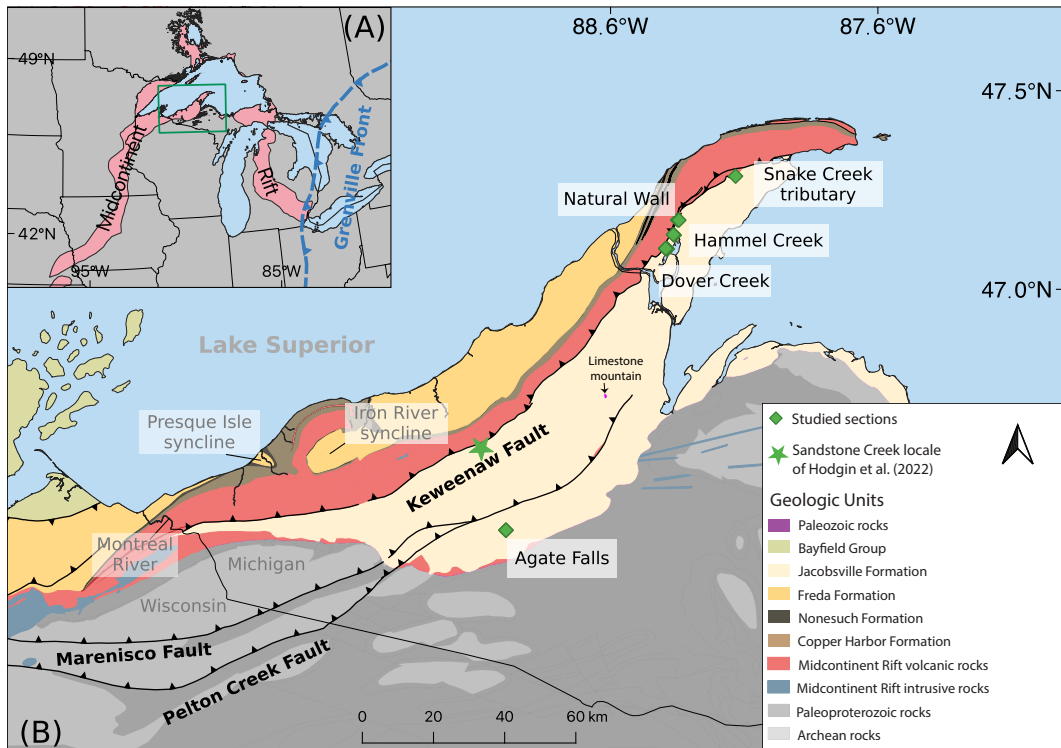


Figure 1. (A) Regional map showing the extent of the Midcontinent Rift and the location of the Grenville Front relative to the study area. The inset green box shows the extent of panel B. (B) Geologic map of northern Michigan and Wisconsin showing Midcontinent Rift igneous and sedimentary rocks, sedimentary rocks of the Jacobsville Formation and Bayfield Group, other older Paleoproterozoic and Archean rocks, and major post-rift thrust faults. The location of the Jacobsville stratigraphic sections in this study are shown with green diamonds. Map modified from Nicholson et al. (2004).

73 Paleomagnetic poles can also be developed from sedimentary rocks deposited in basins.
 74 Sedimentary rocks of the Oronto Group deposited during post-rift thermal subsidence
 75 following the bulk of Midcontinent Rift magmatic activity provide paleomagnetic poles
 76 that extend the Keweenawan Track to ca. 1070 Ma (Henry et al., 1977; Slotznick et al.,
 77 2023). While there are some contemporaneous basins in northern Laurentia (Greenman
 78 et al., 2021), there is minimal basin development within Laurentia following the Grenvillian
 79 orogeny until the Rodinia supercontinent began to rift apart ca. 770 Ma (Macdonald
 80 et al., 2023).

81 One rare preservation of an early Neoproterozoic sedimentary succession in Lau-
 82 rentia's interior is the Jacobsville Formation (Fig. 1; Hamblin (1958); Hodgin et al. (2022);
 83 DeGraff and Carter (2022)). U-Pb detrital zircon dates developed through chemical abra-

84 sion–isotope dilution–thermal ionization mass spectrometry (CA-ID-TIMS) of 1003.21
 85 \pm 2.23 Ma and 992.51 \pm 0.64 Ma (2σ analytical uncertainty) constrain the maximum de-
 86 position age of the Jacobsville Formation (Hodgin et al., 2022). A 985.5 \pm 35.8 Ma (2σ
 87 analytical uncertainty) U-Pb date from calcite veins within the Keweenaw fault provides
 88 a minimum age constraint on Jacobsville deposition, as the Jacobsville Formation is folded
 89 in the footwall against Midcontinent rift volcanics in the hanging wall. Together, these
 90 dates bracket the depositional age of the Jacobsville Formation and constrain it to be
 91 ca. 990 Ma (Hodgin et al., 2022). These results support the interpretation that the for-
 92 mation was deposited within a syn-orogenic basin during the Rigolet phase of the Grenvil-
 93 lian orogen and was then deformed during the same orogenic phase.

94 The Jacobsville Formation contains abundant hematite-bearing sandstone and silt-
 95 stone which have the potential to record a key pole in Laurentia’s apparent polar wan-
 96 der path (APWP) (Dubois, 1962; Roy & Robertson, 1978). Roy and Robertson (1978)
 97 conducted a paleomagnetic study that developed a pole which has been used in paleo-
 98 geographic syntheses where it has been assigned variable ages including an age of ca. 1020
 99 Ma based on APWP extrapolation (e.g. Li et al., 2008). However, the uncertainty in the
 100 age of the magnetization combined with a lack of field tests, and no application of in-
 101 clination correction have resulted in the pole not being included in recent curated com-
 102 pilations (e.g. Evans et al., 2021). Obtaining high-quality paleomagnetic data, includ-
 103 ing robust field tests, motivates the development of new data from the Jacobsville For-
 104 mation.

105 In this study, we investigate five stratigraphic sections of the Jacobsville Forma-
 106 tion on and near the Keweenaw Peninsula, Michigan, USA (Figs. 1 and 2). These sec-
 107 tions were chosen given the abundance of fine-grained siliciclastic lithologies where mag-
 108 netization can be constrained through intraclast conglomerate field tests. Additionally,
 109 they are within the continuous bedrock belt from which chronostratigraphic constraints
 110 have been developed. In contrast to fluvial sandstones in other exposures such as in the
 111 eastern Lake Superior region near Sault Ste. Marie, the maximum and minimum depo-
 112 sitional ages of these sections can be more confidently constrained.

113 Within sampled lithologies, high-resolution thermal demagnetization isolates pri-
 114 mary detrital remanent magnetization (DRM) from secondary chemical remanent mag-
 115 netization (CRM). This interpretation is supported by the DRM directions passing in-
 116 traformational conglomerate tests on siltstone intraclasts that were ripped-up and re-
 117 mobilized within the fluvial depositional environment. A paleomagnetic fold test further
 118 constrains the timing of DRM acquisition to predate the folding of the Jacobsville For-
 119 mation in the footwall of the Keweenaw Fault soon after deposition. With these data,
 120 we develop a new inclination-corrected paleomagnetic pole for the Jacobsville Forma-
 121 tion based on a large number of samples that gives new constraints on the paleogeographic
 122 position of Laurentia in the earliest Neoproterozoic.

123 Geologic setting

124 The ca. 1109 Ma to 1084 Ma North American Midcontinent Rift is a major intra-
 125 continental rift system that extends over 2000 km through the Laurentia craton (Fig.
 126 1). Following the end of active extension in the rift, thermal subsidence resulted in the
 127 accumulation of >4 km of ca. 1085–1050 Ma Oronto Group strata that are both inter-
 128 calated with the youngest volcanics and deposited atop them (Fig. 1; Daniels (1982);
 129 Cannon (1989)). Subsequently, the rift was inverted as contraction associated with the
 130 ca. 1090–980 Ma Grenvillian Orogeny on the eastern margin of Laurentia (Fig. 1) prop-
 131 agated into Laurentia’s interior (Cannon et al., 1993; Cannon, 1994; Hodgin et al., 2022;
 132 Swanson-Hysell et al., 2023).

During rift inversion, Midcontinent Rift volcanic and sedimentary rocks were uplifted along with Paleoproterozoic and Archean lithologies via thrust faults such as the Marenisco fault, forming the crustal-scale Montreal River monocline (Fig. 1; Cannon et al. (1993)). Rb-Sr biotite thermochronology data of Cannon et al. (1993) show Archean lithologies within the Montreal River monocline to have been exhumed to mid to shallow crustal temperatures ($\sim 270^{\circ}\text{C}$) by ca. 1050 Ma. The Jacobsville Formation overlies an angular unconformity that developed on lithologies that were exhumed through this earlier episode of contractional deformation associated with Grenvillian orogenesis (Fig. 1; Hamblin (1958); Cannon et al. (1993); Kalliokoski (1982)). Conglomeratic facies occur in the basal Jacobsville Formation, with clasts derived from locally uplifted basement lithologies (Irving & Chamberlin, 1885; Hamblin, 1958; Kalliokoski, 1982).

Bedding planes in the Jacobsville Formation typically have shallow dips. The exception to these near-horizontal orientations is proximal to reverse faults such as the Keweenaw fault (Fig. 1) where the Jacobsville Formation was occasionally deformed into monoclinal drag folds resulting in steeply tilted to overturned beds (Fig. 1; Irving and Chamberlin (1885); Cannon and Nicholson (2001)). Recent mapping of the Jacobsville Formation also found that it sometimes onlaps the Midcontinent Rift volcanics within or adjacent to en echelon fault branches of the Keweenaw fault system near the northern end of the Keweenaw Peninsula (Tyrrell, 2019; Mueller, 2021). These observations are consistent with the interpretation that there was deposition of Jacobsville Formation sediments during faulting.

Overview of Jacobsville sedimentology and stratigraphy

The Jacobsville Formation is a fluvial succession of feldspathic and quartzose conglomerates, sandstones, siltstones, and shales devoid of lava flows or cross-cutting igneous dikes although internal clastic dikes are present (Hamblin, 1958). Sandstones of the Jacobsville Formation are more quartz-rich with generally fewer lithic fragments than sandstones of the Oronto Group such that they can typically be classified as subarkose to quartz arenites (Fig. 3; Hamblin (1958); Ojakangas and Dickas (2002)). While much of the Jacobsville Formation is dominated by sandstone channel deposits, there are clay-rich siltstones that formed in overbank settings that are a major focus of this study.

In southern exposures of the Jacobsville Formation, conglomerate facies typically have provenance sourced from Paleoproterozoic lithologies such as vein quartz and iron formation clasts (Hamblin, 1958; Kalliokoski, 1982). The occurrence of these conglomerates in proximity to the Marenisco fault and Pelton Creek fault and the downsection steepening of stratal dips interpreted as growth strata may represent syn-depositional development of local relief (Fig. 1; Kalliokoski (1982); Hedgman (1992)). Close to the Keweenaw fault in the central Keweenaw Peninsula (Fig. 1), the Jacobsville Formation consists dominantly of quartz-rich, trough cross-bedded, medium-grained sandstone, with locally abundant clast-supported pebble to cobble conglomerate, and interbeds of red, hematite-bearing, micaceous siltstone to fine-grained sandstone (Dover Creek, Hammel Creek, Natural Wall; Figs. 2 and 3). In this region, the conglomerate contains abundant rounded to angular volcanic clasts as large as boulders that are likely derived from uplifted Midcontinent Rift volcanics (Irving & Chamberlin, 1885; Brojanigo, 1984). Thicker intervals of dark red to brick red siltstone and very fine-grained sandstone are interbedded with coarser-grained sandstone and conglomerate at Agate Falls and Dover Creek (Figs. 2 and 3). Intraclasts of the siltstones are found within some channelized interbeds of sandstone and conglomerate (Fig. 4).

The abundance of clasts of rift volcanics in the conglomeratic facies at Dover Creek, Hammel Creek, and Natural Wall indicates the presence of uplifted volcanics in proximity to the Keweenaw fault in the central part of the peninsula during Jacobsville deposition (Figs. 1 and 2). Coarse-grained arkosic to lithic sandstone is a facies associated

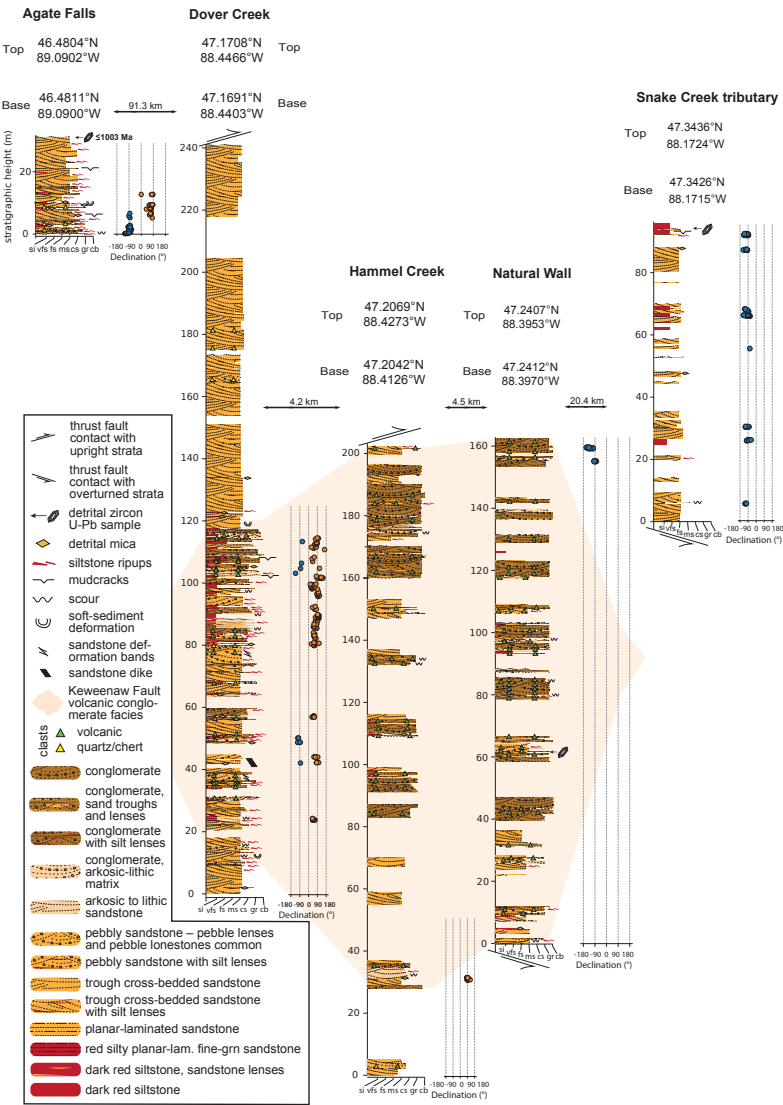


Figure 2. Lithostratigraphy and magnetostratigraphy for studied sections of the Jacobsville Formation in northern Michigan, USA. GPS locations for the base and top of the sections are noted. Paleomagnetic sampling focused on the dark red siltstone to fine-grained sandstone lithofacies. Paleomagnetic specimen declinations are plotted with blue circles corresponding to normal polarity and orange circles to reverse polarity. The maximum depositional age of the Agate Falls section is constrained by a CA-ID-TIMS detrital zircon U-Pb date of 1003.2 ± 2.2 Ma (sample AF1-29.3 of Hodgin et al. (2022)). In the Snake Creek tributary and Natural Wall sections, the position of the detrital zircon samples BSC1-92.5 and NW1-61.5 from Hodgin et al. (2022) are shown. No U-Pb zircon dates from these samples were younger than the age of Midcontinent Rift volcanics. A correlation of a facies association consisting of volcanic-clast conglomerate, coarse arkosic sandstone, and dark red clay-rich siltstone is inferred between the sections at Dover Creek (along Dover Creek and a tributary falls), Hammel Creek, and Natural Wall (Brojanigo, 1984). The stratigraphic correlation between Jacobsville sections at Agate Falls and Snake Creek tributary with these correlated sections from the central Keweenaw Peninsula is relatively uncertain.



Figure 3. Field photos of the Jacobsville Formation. (A) The red/white medium-grained sandstone with decimeter-scale trough cross-stratification in this image (taken at the shore near the unincorporated community of Jacobsville 46.9819°N , 88.4068°W) is a wide-spread lithofacies in the formation, but was not targeted for paleomagnetic sampling in this study. (B, C, D) At the Snake Creek tributary and the Natural Wall ravine in the northeastern Keweenaw Peninsula, intervals of red fine-grained sandstone to siltstone beds can be found through the steeply dipping to overturned basal strata near the Keweenaw fault and also the nearly horizontal upper strata. At the Dover Creek section (E), thick red siltstone horizons interbedded or interfingering with sandstones and conglomerates are found along a Dover Creek tributary waterfall (47.1708°N , 88.4466°W ; this waterfall is distinct, but close to Hungarian Falls). Abundant reoriented siltstone intraclasts can be present within the conglomeratic layers above siltstone beds (Fig. 4). (F) At Agate Falls, nearly flat-lying red fissile siltstone beds are exposed. Detrital mica grains deposited parallel to the bedding plane are often present within the siltstone facies. Another set of siltstone intraclasts were sampled from a conglomeratic layer at Agate Falls for a paleomagnetic conglomerate test (Fig. 4).

184 with the volcanic-clast conglomerates and likely derived from mechanical weathering of
 185 the exhumed volcanics. Chemical weathering of exhumed volcanics from the hanging wall
 186 is a likely source of clay within the abundant fine-grained lithologies that are associated
 187 with the volcanic-clast conglomeratic facies (Fig. 2. Detrital zircon provenance data from
 188 Jacobsville samples on the Keweenaw Peninsula developed by Malone et al. (2020) re-

veal zircon with dates overlapping with Midcontinent Rift volcanism consistent with this provenance interpretation. Detrital mica grains up to ~5 mm in size that are commonly found within siltstone to fine-grained sandstone within the Jacobsville are likely sourced from Paleoproterozoic and Archean lithologies in the region (Fig. 1) and preferentially settled in lower energy overbank settings.

The thickness of the Jacobsville strata can vary in northern Michigan (Hamblin, 1958; Kalliokoski, 1982), and complete stratigraphic sections are not exposed at the studied localities (Figs. 1 and 2). Clay-rich red siltstone is more abundant in conjunction with conglomerates (e.g. 20-120 m in the Dover Creek section; Figs. 2 and 3) than with the cross-stratified sandstone which dominates much of the formation. Relatively thin lithic to arkosic sandstone beds, which are otherwise uncommon in the Jacobsville Formation, are commonly associated with the volcanic conglomerates and red siltstones near the Keweenaw Fault (Fig. 2). Together, the volcanic conglomerates, red siltstones, and arkosic sandstones make up a unique facies association. As previously interpreted by Brojanigo (1984), this facies association was likely deposited proximal to actively uplifting volcanic rocks near the Dover Creek, Hammel Creek, and Natural Wall sections (Fig. 2). The relative stratigraphic positions of the Agate Falls and Snake Creek tributary sections are less certain (Figs. 1 and 2).

The Jacobsville Formation has been mapped to have a continuous extent from the Wisconsin and Michigan border northeast to the Keweenaw Peninsula and east to the Marquette region (Fig. 1; Hamblin (1958); Cannon et al. (1995, 1996); Cannon and Nicholson (2001)). In the eastern Lake Superior region near Sault Ste. Marie, Ontario, there are exposures of sedimentary rocks that are also mapped as the Jacobsville Formation (Hamblin, 1958). As observed on the Keweenaw Peninsula, these sandstones are within the footwall of faults where they are overthrust by Midcontinent Rift volcanics near Mamainse Point (Manson & Halls, 1994). To the west, the Jacobsville Formation has been interpreted to be correlative with sedimentary rocks of the Bayfield Group in northern Wisconsin and the Fond du Lac Formation and Hinckley Formation in Minnesota (Thwaites, 1912; Hamblin, 1958; Wallace, 1971; Kalliokoski, 1982; Ojakangas et al., 2001). A challenge associated with these correlations is that the ca. 1075 to 1050 Ma Freda Formation of the Oronto Group and the ca. 990 Ma Jacobsville Formation have quite similar fluvial lithofacies despite being deposited in distinct basinal settings at different times.

221 Paleomagnetic results and interpretation

Oriented paleomagnetic samples were collected with a portable electric drill from five stratigraphic sections of the Jacobsville Formation in northern Michigan (Figs. 1 and 2). Additional oriented cores and block samples of siltstone intraclasts within conglomerates and conglomeratic sandstones were sampled within the Dover Creek and Agate Falls sections (Figs. 1 and 2, and 4). To maximize sampling of distinct time snapshots of the geomagnetic field at the time of Jacobsville deposition and average out paleosecular variation, we optimized for vertical stratigraphic coverage (Sapienza et al., 2023). Each sample is a distinct stratigraphic horizon and therefore a paleomagnetic site, representing a unique record of the geomagnetic field. Red fine-grained sandstone to shaly siltstone layers were preferentially sampled as they have lower permeability and are less susceptible to diagenetic alteration through fluid flow than coarser-grained sandstone. These fine-grained lithologies are typically of deep red color in contrast to coarse-grained lithologies that have splotchy tan, red, and light green coloration associated with secondary reduction (Fig. 3A). Care was taken to avoid collecting samples with reduction spots. Paleomagnetic cores and blocks were oriented using a magnetic compass and a sun compass when possible. Sun compass data were preferentially used when available. A total of 379 specimens including 30 intraclasts were collected for paleomagnetic study. To minimize the visual impact of sampling, rock containing core holes was knocked out

240 of outcrops following samples—readily done for the friable siltstones and sandstones of
 241 the Jacobsville Formation.

242 Challenges exist in isolating the primary magnetization in sedimentary rocks. Primary
 243 detrital remanence acquired during deposition can be masked by secondary rema-
 244 nence acquired through precipitation and growth of diagenetic minerals within sedimen-
 245 tary rocks syn- to post-deposition (e.g. pigmentary hematite formed from precursor phases
 246 such as ferrihydrite; Jiang et al. (2018)). In red beds, it has been found that formation
 247 of pigmentary hematite can post-date the timing of deposition, resulting in a chemical
 248 remanent magnetization superimposed upon primary detrital remanent magnetization
 249 carried by detrital grains (Collinson, 1974; Tauxe et al., 1980). To isolate the remanence
 250 components of sandstones of various grain sizes of the Jacobsville Formation, Roy and
 251 Robertson (1978) adopted a method first applied by Collinson (1965) to preferentially
 252 remove fine-grained pigmentary hematite through prolonged immersion in concentrated
 253 HCl acid. Progressively longer immersion times first dissolve the nanometer-scale pig-
 254 mentary hematite prior to dissolving the coarser micrometer-scale detrital grains. Stud-
 255 ies applying paired acid etching demagnetization and thermal demagnetization show that
 256 the pigmentary hematite grains tend to have lower unblocking temperatures than de-
 257 trital ones (Tauxe et al., 1980; Bilardello & Kodama, 2010). High-resolution thermal de-
 258 magnetization experiments with temperature intervals as small as 1-2 °C have also been
 259 shown to be effective in isolating detrital remanence from chemical remanence as coarser
 260 hematite grains tend to have higher unblocking temperatures closer to the Néel temper-
 261 ature of hematite (Jiang et al., 2015; Swanson-Hysell, Fairchild, & Slotznick, 2019).

262 In the Jacobsville Formation samples that we collected, there are both detrital hematite
 263 grains (10s of micrometers) as well as finer grained (sub-micrometer) pigmentary hematite
 264 (Fig. S1). We adopted a thermal demagnetization protocol with increasingly higher res-
 265 olution approaching the Néel temperature of hematite (5 °C to 2 °C; Fig. 4, S2). The
 266 specimens underwent stepwise thermal demagnetization at the UC Berkeley Paleomag-
 267 netism Lab using an ASC demagnetizer (residual fields <10 nT) with measurements made
 268 on a 2G DC-SQUID magnetometer. Due to the thermal gradient in the oven, we keep
 269 the specimens at the same location throughout the demagnetization steps. This proto-
 270 col makes the temperature difference between each step relatively consistent for each spec-
 271 imen compared to if they changed positions within the oven. While the very fine-grained
 272 sandstone and siltstone lithologies typically do not have an appreciable present-day lo-
 273 cal field overprint component, such a component can be present in fine-grained sandstones
 274 and is removed by ~300°C during thermal demagnetization (Fig. S2, S3). A total of 356
 275 specimens yielded detrital remanent magnetizations that can be fit with least-square lines
 276 (Kirschvink, 1980). These fits were made using PmagPy (Tauxe et al., 2016) and all pa-
 277 leomagnetic data are available to the measurement level in the MagIC database (<https://10.7288/V4/MAGIC/19780>).

279 Paleomagnetic field tests

280 *Fluvial intraclast conglomerate tests*

281 Similar to the thermal demagnetization results of the hematite-bearing fluvial in-
 282 traclasts of the Freda Formation (Swanson-Hysell, Fairchild, & Slotznick, 2019), the silt-
 283 stone intraclasts of the Jacobsville Formation typically reveal two distinct magnetiza-
 284 tion components (Fig. 4). One component shows similar vector orientations amongst in-
 285 traclasts and was typically removed up to 640-655 °C (Fig. 4). The relatively low un-
 286 blocking temperatures and similarity in directions among the reoriented intraclasts in-
 287 dicate that it is chemical remanent magnetization acquired through crystallization of sec-
 288 ondary pigmentary hematite following clast redeposition. After removal of this compo-
 289 nent, further thermal demagnetization with small step increments at higher tempera-
 290 tures up to ~689 °C often reveal an origin-trending component (Fig. 4). In the data from

291 the clasts, there is typically a significant directional change in specimen magnetization
 292 between the mid-temperature component and the high-temperature component. As a
 293 result, 27 out of 30 intraclast specimens could be fit with high-temperature least squares
 294 lines. Distinct from the well-grouped mid-temperature component directions, the high-
 295 temperature directions of the intraclasts are dispersed and the null hypothesis of ran-
 296 domness cannot be rejected at the 95% confidence level ($n=5$ for intraclasts at Agate Falls
 297 and $n=22$ for intraclasts at Dover Creek; Fig. 4; Watson (1956)). This result indicates
 298 that the high unblocking temperature remanence is primary and was acquired by detri-
 299 tal hematite grains during initial deposition prior to the clasts being ripped up and re-
 300 oriented within the depositional environment. This conglomerate test provides strong
 301 support for interpreting the high unblocking temperature remanence in the *in situ* beds
 302 as a primary DRM.

303 ***Fold test***

304 A total of 71 specimens yielded interpretable DRM directions throughout the strati-
 305 graphic section at the Snake Creek tributary (Figs. 1 and 6). The stratigraphic section
 306 is within a large-scale drag fold within the immediate footwall of the Keweenaw fault.
 307 As a result, there are exposures of steeply tilted, moderately tilted, as well as nearly hor-
 308 izontal beds along this section that allow us to conduct a paleomagnetic fold test to in-
 309 vestigate the timing of magnetization. The chronological constraints on the timing of
 310 Keweenaw fault motion indicate that the folding occurred on a timescale of ~ 10 Myr of
 311 deposition—making this fold test a more informative constraint on the age of the rema-
 312 nance than typical for such tests. Given that the more steeply tilted beds accommodated
 313 deformation during shortening associated with the Keweenaw fault motion, they could
 314 be more prone to non-cylindrical folding and complicate tilt-correction of the paleomag-
 315 netic directional data (e.g. Pueyo et al., 2003; Nabavi & Fossen, 2021). Therefore, we
 316 conduct a paleomagnetic bootstrap fold test (Tauxe & Watson, 1994) using specimens
 317 from the nearly horizontal beds and the moderately tilted beds. The results show that
 318 the degrees of untilting that result in the best grouping of the DRM directions have 95%
 319 confidence bounds that overlap with 100% unfolding, consistent with the specimens hav-
 320 ing acquired their magnetization prior to tilting (Fig. 5). This positive fold test further
 321 supports the interpretation that the Jacobsville red beds acquired a primary detrital rema-
 322 nance during deposition. In contrast, the mid-temperature component directions that
 323 typically unblock up to 650 °C from the Snake Creek tributary fail a fold test (Fig. S4),
 324 consistent with them being acquired as chemical remanent magnetizations that postdate
 325 the tilting. The positive fold test on the detrital remanence in combination with the sim-
 326 ilarity of the detrital and chemical remanence directions (Fig. 6B) indicates that the ma-
 327 jority of chemical remanence acquisition likely occurred geologically soon after the de-
 328 formation.

329 **Paleomagnetic reversals**

330 With the insights gained from the thermal demagnetization results of the Jacob-
 331 sville fluvial intraclasts and the fold test (Figs. 4 and 5), we next investigate the detri-
 332 tal remanent magnetizations for all *in situ* specimens from the five stratigraphic sections
 333 (Figs. 1 and 2). The DRM directions are plotted by stratigraphic section location in Fig-
 334 ure 6. As observed in the sparser data of Roy and Robertson (1978), there are dual po-
 335 larity magnetizations (Fig. 2). The paleomagnetic polarity reversals are shown in strati-
 336 graphic context in Figure 2 with specimen magnetization declinations plotted against
 337 stratigraphic heights. The record of Laurentia's paleomagnetic poles from the Protero-
 338 zoic through the Phanerozoic (see compilations in Torsvik et al. (2012) and Swanson-
 339 Hysell (2021)) gives a continuity of the orientation of the continent that enables the geo-
 340 magnetic polarity of the directions to be interpreted. In this framework, the westerly

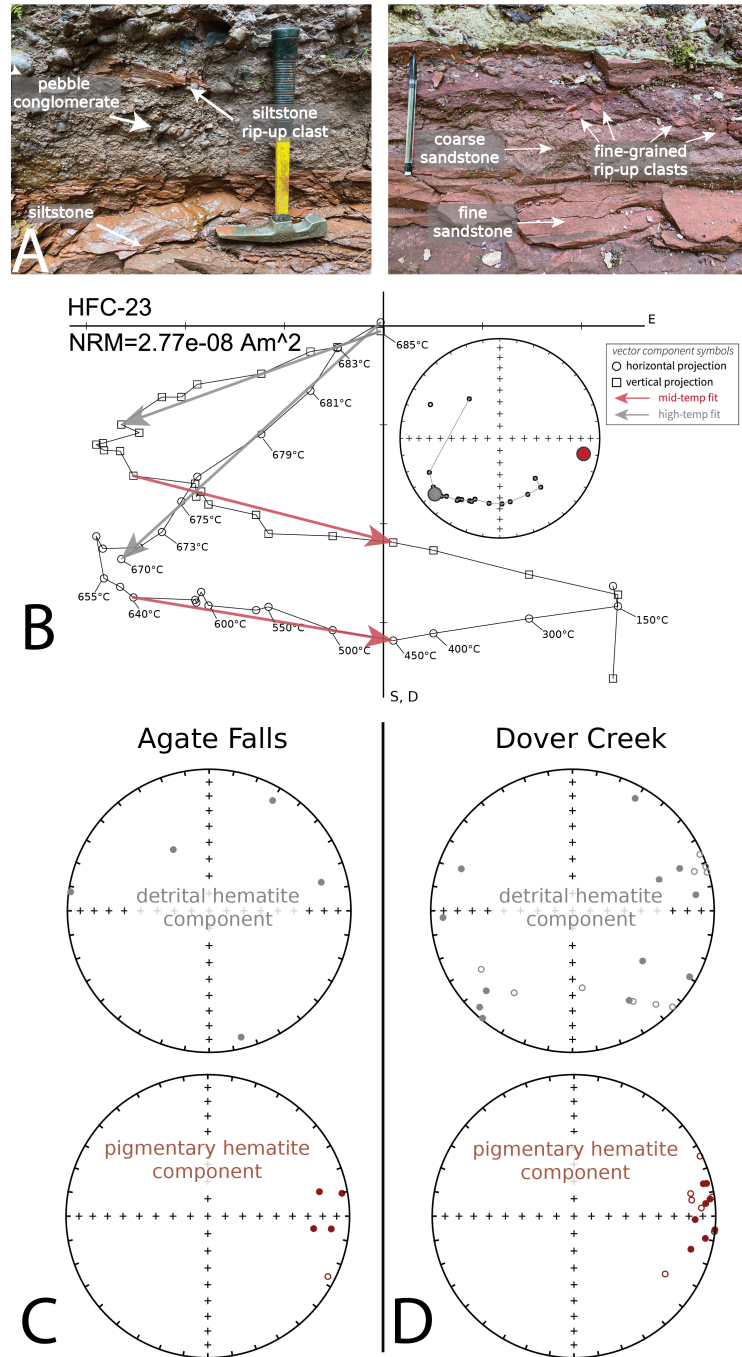


Figure 4. (A) Field photos of siltstone to fine-grained sandstone fluvial intraclasts within conglomerate and conglomeratic sandstone beds in the Jacobsville Formation. (B) Representative step-wise thermal demagnetization data from an intraclast from Dover Creek (HFC-23) plotted on an orthogonal vector diagram. The plot reveals a mid-temperature component and an origin-trending high-temperature component. The components are present as varying fractions of the overall remanence in different specimens. The direction of the mid-temperature component (interpreted as secondary CRM) is shown as dark red arrows on the orthogonal vector plots and dark red circles on the equal area plots, while the high-temperature component (interpreted as primary DRM) is shown in grey. (C, D) The mid-temperature component has a similar direction among the clasts as can be seen on the summary equal area plots. In contrast, the high-temperature component directions are dispersed and pass the randomness test of Watson (1956). Both the DRM and the CRM directions are shown in geographic coordinates. NRM = natural remanent magnetization.

341 DRM directions are normal geomagnetic polarity and the easterly DRM directions are
 342 reversed polarity (Fig. 6).

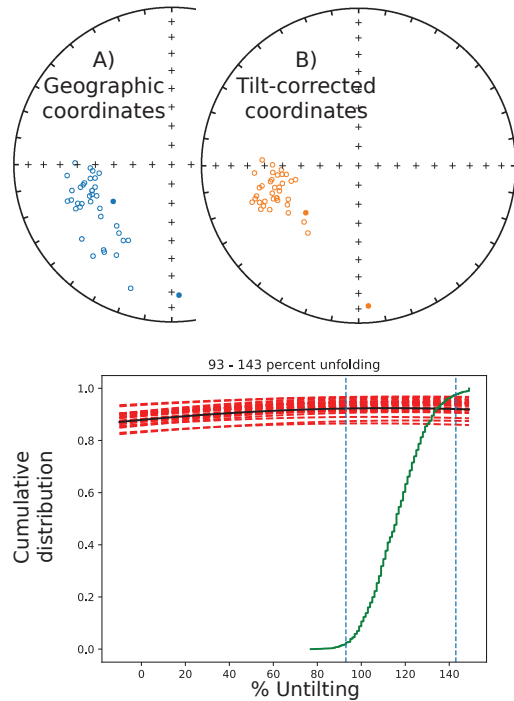


Figure 5. Bootstrap paleomagnetic fold test (Tauxe & Watson, 1994) of the detrital remanent magnetization directions recorded by specimens from the nearly horizontal beds and moderately tilted beds at the Snake Creek tributary. Complete unfolding lies within the 95% confidence limits of the test, consistent with the magnetization having been acquired prior to tilting.

At the Dover Creek section, which goes along Dover Creek and then up the waterfall of a side tributary (the Hungarian Falls side falls), numerous hematite-rich siltstone to fine sandstone layers commonly occur in association with trough cross-bedded sandstone and conglomeratic facies. These lithofacies are particularly well-exposed along a tributary waterfall to Dover Creek such that 158 samples were collected for paleomagnetic study (Fig. 1, 2), making this section the most densely sampled amongst all the sections. The specimen DRMs show that the geomagnetic field reversed at least nine times during deposition within the section (Fig. 2).

The Natural Wall and Hammel Creek sections are in close proximity to the Dover Creek section (Fig. 1) and the unique sedimentary facies association of volcanic-clast conglomerate, red siltstone, and coarse arkosic sandstone is similar to the basal ~120 meters of the section at Dover Creek (Fig. 2). Our sampling at these two localities is more limited due to there being poorer exposures of siltstone and fine-grained sandstone beds in these sections (Fig. 2). At Hammel Creek, 16 samples from two siltstone layers near the base of the section are of reversed polarity (Fig. 2). Near the top of the Natural Wall section, consistent normal-polarity directions are recorded by 15 samples (Fig. 2).

At the Snake Creek tributary (Fig. 1), 71 specimens yielded interpretable DRMs through multiple levels along the ~95-meter-thick section and all show normal-polarity directions (Figs. 6 and 2). At Agate Falls (Fig. 1), clay-rich detrital mica-bearing siltstone layers occur through ~30 meters of strata that are incised by the Middle Branch Ontonagon River (Fig. 3). 67 total paleomagnetic samples were collected on both sides of the waterfall (Fig. 2). At least three geomagnetic polarity reversals occurred during deposition within the Agate Falls section (Fig. 2).

The paleomagnetic reversal test assesses whether two directional data sets share a common mean when one of the polarity directions is flipped to its antipode. Although the occurrence of multiple geomagnetic field reversals during deposition of the Jacobsville Formation is evident (Figs. 2 and 6), the limited and often discrete records of many polarity chronos are insufficient for pair-wise reversal tests within single sections (Fig. 2).

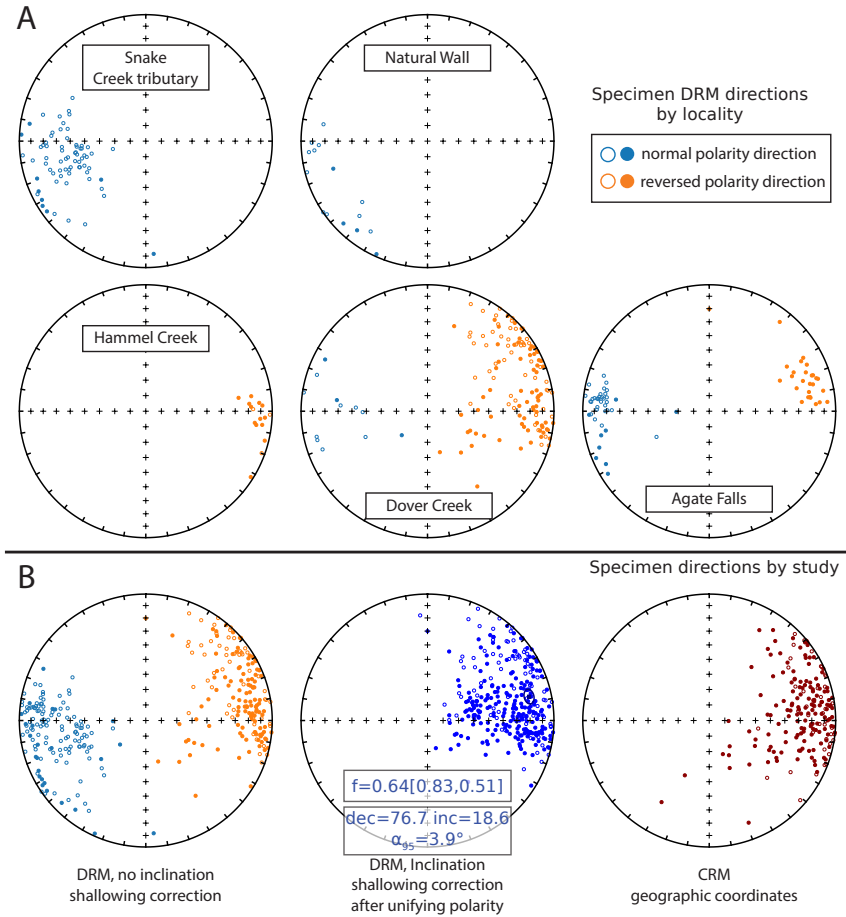


Figure 6. (A) Specimen detrital remanence directions (DRM) plotted by locality on equal area plots. During sample collection, we optimized for vertical stratigraphic coverage such that each sample constitutes a single horizon and therefore a paleomagnetic site. Specimens from the Snake Creek tributary as a mean direction of $\text{dec}=256.0^\circ$, $\text{inc}=-30.5^\circ$, $k=9.9$, $\alpha_{95}=5.6^\circ$, $n=71$; the Natural Wall section has a mean direction of $\text{dec}=242.4^\circ$, $\text{inc}=-6.4^\circ$, $k=9.0$, $\alpha_{95}=13.5^\circ$, $n=15$; the Hammel Creek section has a mean direction of $\text{dec}=94.1^\circ$, $\text{inc}=8.7^\circ$, $k=30.7$, $\alpha_{95}=6.8^\circ$, $n=16$; the Dover Creek section has a mean direction of $\text{dec}=73.2^\circ$, $\text{inc}=5.4^\circ$, $k=5.6$, $\alpha_{95}=5.6^\circ$, $n=138$; the Agate Falls section has a mean direction of $\text{dec}=83.4^\circ$, $\text{inc}=13.0^\circ$, $k=13.4$, $\alpha_{95}=4.9^\circ$, $n=67$. All reported directions are calculated in tilt-corrected coordinates and after unifying polarity. The measurement-level data are available in the MagIC database (<https://10.7288/V4/MAGIC/19780>). (B) Summary equal area plots at the study-level combining directions from all localities. The elongation/inclination (E/I) method (Tauxe & Kent, 2004) was used to estimate the amount of inclination shallowing in Jacobsville specimen DRMs after unifying the polarities (flipping the normal [blue] directions to their antipodes). Details on inclination shallowing corrections are shown in Figure 7 with the value of $f=0.64$ used for the directions in the middle panel. All DRM directions are shown in tilt-corrected bedding coordinates. The summary plot of all specimen chemical remanence directions (CRM) are shown in geographic coordinates show well-grouped reversed-polarity directions whose directions are similar to the DRMs.

Sedimentation within individual siltstone horizons was likely quite rapid given their deposition within fluvial floodplains potentially without sufficient time to average out secular variation within discrete siltstone intervals. We combine all normal and reversed directions from the five sections and perform a reversal test. The McFadden and McElhinny (1990) reversal test results show the angle between the two mean directions (15.9° ; no inclination shallowing correction) exceeds the critical angle (7.5°) (Fig. S5), thereby

failing the test. This difference largely arises due to normal (west directed) directions in the Snake Creek tributary section being slightly steeper in their upward inclination. There are at least four possible explanations for this behavior: 1) the lower number of normal directions which dominantly come from the Snake Creek tributary section may not have averaged out secular variation; 2) there could have been plate motion during Jacobsville deposition with the normal polarity in the Snake Creek tributary section being acquired when Laurentia was at a slightly higher latitude; 3) there could be a bias from the reversed CRM superimposed on the normal DRM in the Snake Creek tributary specimens being incompletely removed during thermal demagnetization; 4) the geomagnetic field in the early Neoproterozoic could have been slightly different than that of more recent times in terms of the dispersion of pole position at distinct time snapshots potentially associated with changes in field intensity. Regardless, the positive intraclast conglomerate test gives confidence that the Jacobsville Formation has a primary detrital remanent magnetization that can be isolated through thermal demagnetization. This result is strengthened through the positive fold test and the broadly antipodal dual polarity data. Additionally, taking the large number of samples together from both polarities to calculate a pole increases the likelihood that the dual polarity pole has averaged out secular variation.

A total of 186 specimens yielded interpretable chemical remanence directions that are of dominantly reversed polarity. These directions are plotted by stratigraphic section location in Figure S6 and are all shown in Figure 6B. That the CRM directions are a secondary remanence component that postdate the deposition of the Jacobsville Formation is supported by the negative intraformational conglomerate test results and failure in the fold test (Figs. 4, S4). However, the similarity of the CRM directions (declination=96.2°, inclination=15.1°, $\alpha_{95}=4.2^\circ$, n=186) with the primary DRM directions (declination=103.1°, inclination=13.4°, $\alpha_{95}=3.3^\circ$, n=307, no inclination shallowing correction) indicate that growth of the secondary pigmentary hematite which carries the CRM likely occurred soon after deposition when Laurentia was in a similar paleogeographic position.

Overall, the multiple geomagnetic field polarity reversals recorded by the Jacobsville Formation constrain that the end of the Keweenawan normal superchron (Driscoll & Evans, 2016) (which started ca. 1099 Ma; Swanson-Hysell, Ramezani, et al. (2019)) had to have ended by the onset of Jacobsville deposition.

410 Discussion

411 Averaging paleosecular variation and correcting for inclination shallow- 412 ing

Igneous and sedimentary rocks associated with the North American Midcontinent Rift provide a high-resolution record of the ca. 1109 to 1070 Ma Keweenawan Track which tightly constrains the apparent polar wander path for Laurentia in the late Mesoproterozoic (Fig. 8; Swanson-Hysell, Ramezani, et al. (2019)). However, high-quality paleogeographic constraints thereafter are sparser and more uncertain in their age until the ca. 775 Ma Gunbarrel large igneous province (Harlan et al., 2003) and subsequent ca. 775-719 Ma poles from western Laurentia extensional basins (Weil et al., 2006; Eyster et al., 2019). Developing a new paleomagnetic pole from the Jacobsville Formation presents an opportunity for a well-constrained early Neoproterozoic constraint on Laurentia's paleogeographic position.

Our high-resolution thermal demagnetization successfully isolated detrital magnetization from the secondary chemical magnetization carried by pigmentary hematite that grew after deposition of the Jacobsville Formation. The scatter in the DRM directions can be interpreted to reflect variations in the geomagnetic field during the deposition of

427 the sediments (Steiner, 1983; Tauxe & Kent, 1984). The multiple geomagnetic field re-
 428 versals captured by specimens collected from the Dover Creek and Agate Falls sections
 429 support that a prolonged period of time is represented by the specimens given that the
 430 duration of geomagnetic polarity chronos are typically on the order of tens of Kyr to Myr
 431 timescales (Fig. 2). Therefore, we combine all specimen detrital remanent magnetiza-
 432 tions to calculate a paleomagnetic pole for the Jacobsville Formation.

433 A challenge in interpreting detrital magnetizations is the issue of correcting for in-
 434 clination shallowing (King, 1955; Tauxe & Kent, 2004; Bilardello, 2016). Scatter of the
 435 specimen detrital remanence directions in tilt-corrected coordinates show elongation par-
 436 allel to the bedding plane, consistent with them being shallowed (Fig. 6; Tauxe and Kent
 437 (2004)). Such a directional distribution is due to rotation of detrital hematite grains dur-
 438 ing deposition and subsequent compaction, resulting in inclinations recorded by sedimen-
 439 tary rocks having shallower angles than the local field in which they are deposited. If
 440 uncorrected, shallower inclinations obtained from sedimentary rocks can result in erro-
 441 neously low estimates of paleolatitudes, biasing paleogeographic reconstructions. To es-
 442 timate the amount of inclination shallowing, we apply the statistical elongation/inclination
 443 (E/I) method that evaluates the deviation of the distribution of a large number (>100)
 444 of observed sedimentary paleomagnetic directional data with the predicted distribution
 445 given by a statistical paleosecular variation model (Tauxe & Kent, 2004). Although the
 446 TK03 paleosecular variation model is based on data of relatively recent geomagnetic field
 447 variations, it has been shown to be compatible with data from the ca. 1.1 Ga lava flows
 448 of the Midcontinent Rift (Tauxe & Kodama, 2009). Furthermore, Pierce et al. (2022)
 449 showed that applying the E/I method to detrital hematite magnetizations within the ca.
 450 1093 Ma Cut Face Creek Sandstone in the Midcontinent Rift successfully corrects the
 451 shallow paleomagnetic inclinations of the sediments to that of the North Shore Volcanic
 452 Group lava flows that bracket them. Pierce et al. (2022) also developed a method, that
 453 we use here, to represent uncertainties associated with the amount of inclination shal-
 454 lowing into sedimentary paleomagnetic pole positions which can then be summarized with
 455 an elliptical Kent distribution (Kent, 1982) rather than a circular Fisher distribution (Fisher,
 456 1953).

457 Applying the E/I method to the Jacobsville DRM directions results in an estimate
 458 for the flattening factor (f factor) of 0.64 with a 95% uncertainty range of 0.83 to 0.51
 459 (Figs. 7). The f factor of 0.64 is close to the value of 0.58 which is the mean of incli-
 460 nation shallowing factors compiled for hematite-bearing rocks in Pierce et al. (2022) (build-
 461 ing on compilations of Bilardello (2016) and Vaes et al. (2021)). The Fisher mean inclination-
 462 corrected detrital remanence mean direction is dec=76.7°, inc=18.6° α_{95} =3.9°. The Fisher
 463 mean inclination-corrected paleomagnetic pole associated with this nominal f factor is
 464 Plon=183.4°E, Plat=16.9°S, A_{95} =3.1°. We apply the method of Pierce et al. (2022) to
 465 incorporate the uncertainty in the E/I estimate of the f factor into the uncertainty of
 466 the paleomagnetic pole (Fig. 7). This uncertainty results in more uncertainty associated
 467 with paleolatitude which for the pole is along the great circle path between the mean pole
 468 position and the locality of the Jacobsville sections. Following Pierce et al. (2022), the
 469 pole can be represented with a Kent distribution 95% confidence ellipse which is: mean
 470 longitude=183.4°E, mean latitude=16.9°S, major axis longitude=255.5°E, major axis lat-
 471itude=45.2°N, major axis magnitude=4.1°, minor axis longitude=108.1°E, minor axis lat-
 472itude=39.9°N, minor axis magnitude=3.1°(Fig. 7; Table 1). This pole position is close
 473 to the end of the Keweenawan Track (Fig.8) and far away from Laurentia's pole posi-
 474 tions during the Paleozoic when there was orogenesis along Laurentia's eastern margin
 475 (Fig. S7). This pole position is consistent with the geochronology constraints on the de-
 476 position of the Jacobsville Formation and the positive paleomagnetic field tests that the
 477 detrital remanence of the Jacobsville Formation was acquired during the earliest Neo-
 478 proterozoic.

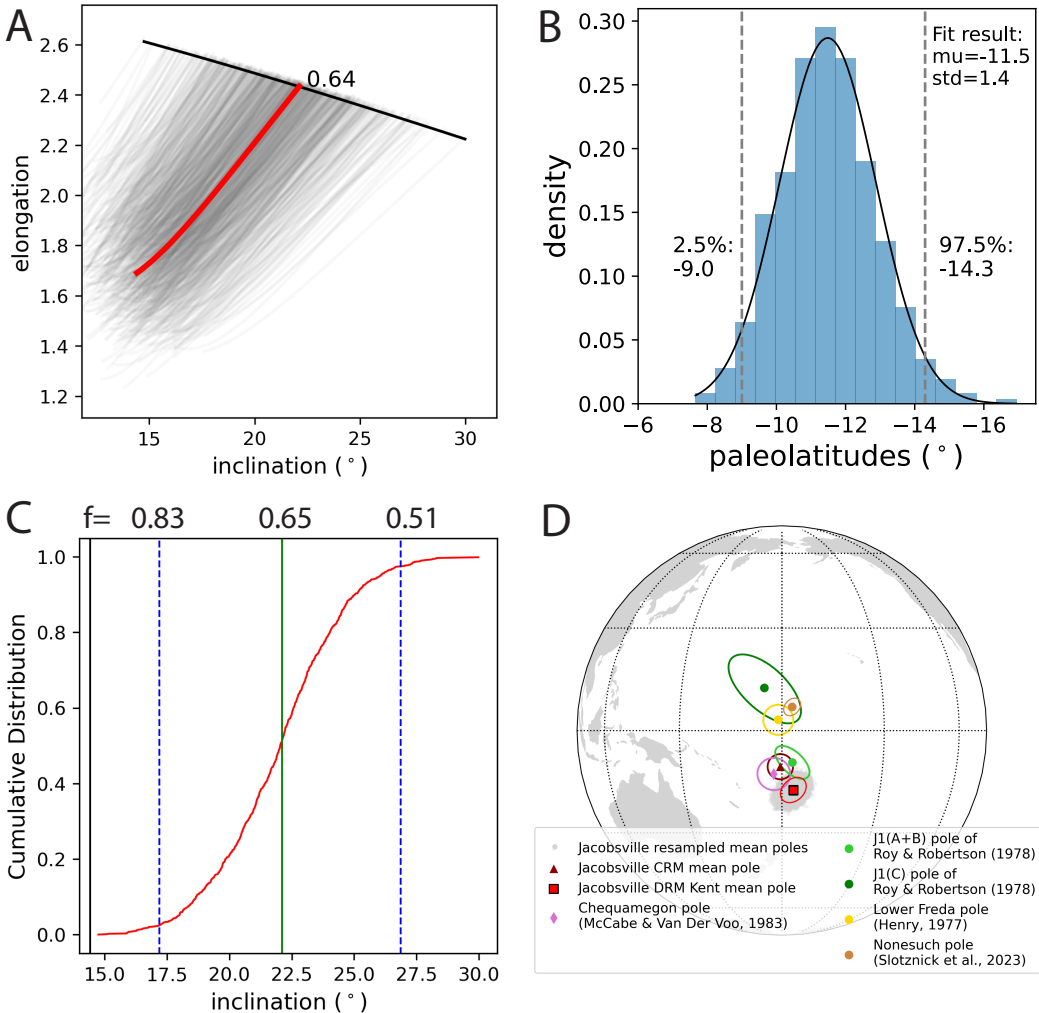


Figure 7. Results of the estimated amount of inclination shallowing of the detrital remanent magnetization of the Jacobsville Formation using the elongation/inclination (E/I) method (Tauxe & Kent, 2004). (A) The E/I method gives an estimated flattening factor $f=0.64$ (red curve) based on where the elongation/inclination curve of the dataset intersects that predicted by the TK03 paleosecular variation model (black curve; Tauxe and Kent (2004)). The grey lines show 1,000 bootstrap resamples of the DRM directions which provide an estimate of the uncertainty associated with the f factor estimate (95% interval from 0.83 to 0.51). (B) The distribution of the paleolatitudes resulting from the corrected inclinations of the E/I bootstrap resamples. That the distribution is drawn from a normal distribution with a mean of -11.5° and standard deviation of 1.4 cannot be rejected in the Kolmogorov-Smirnov test. The 95% confidence bounds shown by dashed lines span a range of paleolatitudes that need to be incorporated into the uncertainty of the reported paleomagnetic pole. (C) The cumulative distribution of inclinations based on the E/I bootstrap results with the 95% confidence bounds shown in terms of inclination and f factor. (D) The new Kent mean inclination corrected DRM pole (red square) of the Jacobsville Formation is shown in the context of the pole calculated for the CRM (purple triangle) as well as the Jacobsville pole developed by Roy and Robertson (1978), the Chequamegon Formation pole of McCabe and Van der Voo (1983), and poles from the Oronto Group (Nonesuch Formation, Slotznick et al. (2023); Freda Formation, Henry et al. (1977)). The mean pole position of the Kent distribution was calculated following the method of Pierce et al. (2022). The close proximity between Jacobsville poles with the Chequamegon pole is consistent with their deposition being coeval. In contrast, the J1 (C) pole of Roy and Robertson (1978) developed from hematite-bearing sedimentary rocks in the Sault Ste Marie region plots in the northern hemisphere close to the Freda Formation pole.

Roy and Robertson (1978) also studied the paleomagnetism of sedimentary rocks grouped as the Jacobsville Formation and isolated a characteristic magnetization component via alternating-field, thermal, and chemical demagnetization on a suite of Jacobsville red beds near the Keweenaw Peninsula (their area A), the town of Marquette (their area B), and Sault Ste Marie (their area C). Although least-squares principal component analyses was not a routine approach in fitting paleomagnetic directions at the time,

Table 1. Kent mean paleomagnetic pole for the Jacobsville Formation

pole	mean pole position (Plon/Plat)	major axis	major axis 95% confidence angle	minor axis	minor axis 95% confidence angle
	γ_1	γ_2	ζ_{95}	γ_3	η_{95}
Jacobsville	183.4°E /	255.5°E /	4.1°	108.1°E /	3.1°
E/I corrected	16.9°S	45.2°N		39.9°N	

Notes: The Fisher mean of the Jacobsville detrital remanence paleomagnetic pole without an inclination shallowing correction is Plon=185.5°E, Plat=14.0°S, A₉₅=2.7°; the Fisher mean of the Jacobsville detrital remanence paleomagnetic pole with an inclination shallowing correction of $f=0.64$ is Plon=183.4°E, Plat=16.9°S, A₉₅=3.1°; the Fisher mean of the Jacobsville chemical remanence paleomagnetic pole is Plon=179.6°E, Plat=10.2°S, A₉₅=3.6°

485 that study had success in removing the present day local field overprint and was able to
 486 resolve dual magnetic polarities at one locality. The mean paleomagnetic pole position
 487 calculated from the interpreted primary magnetic remanence from rocks of the Keweenaw
 488 Peninsula and Marquette area (J1 A+B pole; pole longitude=183°E, pole latitude=9°S,
 489 dp=3°, dm=6°; no inclination correction; Fig. 7; Roy and Robertson (1978)) is in the
 490 southern hemisphere and lies close to the mean pole from this study (Fig. 7). However,
 491 their mean pole developed from fine- and medium-grained sandstone near Sault Ste Marie
 492 lies in the northern hemisphere with a pole latitude of 12°N (Fig. 7). Despite the large
 493 uncertainty ellipse associated with this mean pole position, it is distinct from the mean
 494 pole position from the Jacobsville Formation in northern Michigan. Instead, it overlaps
 495 with the Oronto Group paleomagnetic poles of the ca. 1070 Ma lower Freda Formation
 496 and the ca. 1075 Ma Nonesuch Formation (Fig. 7; Henry et al. (1977); Slotnick et al.
 497 (2023)). As suggested by Dubois (1962) and Roy and Robertson (1978), these data sug-
 498 gest that the fluvial red beds in the Sault Ste Marie area that are often taken to be cor-
 499 relative to the Jacobsville Formation (e.g. Malone et al., 2020) are likely time equiva-
 500 lent to sedimentary rocks of the Oronto Group and deposited during post-rift thermal
 501 subsidence.

502 Deposition of Bayfield Group sedimentary rocks in northern Wisconsin (west of the
 503 studied exposures; Fig. 1) has been hypothesized to be coeval with the Jacobsville For-
 504 mation (Hamblin, 1958; Kalliokoski, 1982; Malone et al., 2016). Published low precision
 505 detrital zircon U-Pb dates developed by laser ablation-inductively coupled plasma-mass
 506 spectrometry (LA-ICP-MS) dates are consistent with this interpretation with a maxi-
 507 mum depositional age of ca. 1035 Ma for the Chequamegon Formation of the Bayfield
 508 Group (Craddock et al., 2013). Our updated Jacobsville pole position is close to a pole
 509 developed from the Chequamegon Sandstone of the Bayfield Group (Fig. 7; pole longi-
 510 tude=177.7°E, pole latitude=12.3°S, A₉₅=4.6°; no inclination correction; McCabe and
 511 Van der Voo (1983)). These data are consistent with the Bayfield Group being deposited
 512 within a contiguous syn-orogenic basin with the Jacobsville Formation during the Rigo-
 513 let phase of the Grenvillian orogeny. This interpretation can be evaluated with further
 514 high-precision geochronology focused on the Bayfield Group.

515 Age of the Jacobsville Pole

516 At the western edge of the Jacobsville bedrock belt in northern Michigan, the for-
 517 mation is in angular unconformity with Midcontinent Rift rocks that were uplifted and
 518 tilted prior to Jacobsville deposition (Fig. 1; Hedgman (1992); Cannon et al. (1995)).
 519 Rb-Sr thermochronologic data developed from Paleoproterozoic to Archean lithologies
 520 that were exhumed along the Marenisco Fault along with Midcontinent Rift strata in this

region indicate that this uplift occurred ca. 1050 Ma associated with the Ottawan phase of the Grenvillian orogeny Cannon et al. (1993). Field observations reveal erosional contacts and development of paleosols between the Jacobsville Formation and underlying Midcontinent Rift volcanic rocks at the Sturgeon River within the bedrock belt (Hamblin, 1958; Zbinden et al., 1988). Seismic reflection data beneath Lake Superior have been also been interpreted to indicate that the Jacobsville Formation lies in angular unconformity atop sedimentary rocks of the Oronto Group (Cannon, 1989). This context requires that there was ca. 1050 Ma contractional deformation of Midcontinent Rift strata, erosion of these tilted strata, and renewed subsidence prior to the onset of Jacobsville deposition atop them.

Maximum depositional detrital zircon dates are consistent with this history and provide additional constraints. Hodgin et al. (2022) applied tandem dating where the young population emerging from a large number of low-precision LA-ICP-MS dates are followed by high-precision CA-ID-TIMS analysis. This approach has the advantage of combining the high number of low-precision analyses that can be acquired through LA-ICP-MS with dates developed through CA-ID-TIMS where the deleterious effects of Pb-loss can be mitigated, and more accurate and precise dates can be obtained. These data reveal the youngest zircon at Sandstone Creek near the Keweenaw Fault (Figure 1) to have a date of 992.51 ± 0.64 Ma (2σ analytical uncertainty) and the youngest zircon at Agate Falls (Figure 1) a date of 1003.21 ± 2.23 Ma (2σ). These dates are consistent with the age of syntectonic magmatism in the Grenville orogen associated with the Rigolet phase of the orogeny (e.g. Bussy et al., 1995; Turlin et al., 2019; Jannin et al., 2018) which is a potential source for the grains. Overall, these dates constrain a maximum depositional age of the Jacobsville Formation in the earliest Neoproterozoic.

While there has been recent success in applying tandem detrital zircon data to obtain maximum depositional ages that are close to true depositional ages (Karlstrom et al., 2020), the possibility exists that deposition could significantly postdate the youngest dated detrital zircon. A firm minimum depositional age on the age of the Jacobsville is that it is unconformably overlain by the Cambrian Munising Formation whose base was deposited ca. 501 to 497 Ma during the Dresbachian Stage (the Guzhangian Stage in the modern Cambrian time scale) (Hamblin, 1958; Haddox & Dott, 1990). This unconformity is erosional as it truncates Jacobsville strata and intraformational clastic dikes and can have slight angularity (Hamblin, 1958; Haddox & Dott, 1990). That the Jacobsville Formation is older than the Munising Formation lends tighter constraints than the Cambrian age itself given the evidence discussed above that Jacobsville deposition was syn-orogenic. The only candidate for such orogenesis is the ca. 1010-980 Ma Rigolet phase of the Grenvillian orogeny given that subsequent Paleozoic orogenesis (e.g. the Ordovician Taconic and Carboniferous Alleghanian orogenies) post-dates deposition of the Munising Formation.

That the Jacobsville Formation is folded in the footwall of the Keweenaw fault, beneath the older Midcontinent Rift volcanic rocks in the hanging wall, provides another opportunity to develop a minimum depositional age. Seeking to obtain such a constraint, Hodgin et al. (2022) targeted calcite within a Keweenaw Fault breccia that cross-cuts a dense network of zeolite veins and slickenslides that yielded a U-Pb date of 985.5 ± 35.8 Ma (2σ). While this calcite date has large analytical uncertainty, it indicates that the fault breccia developed associated with the Grenvillian orogeny and it overlaps with the ca. 1010-980 Ma ages of metamorphism associated with the Rigolet phase of the orogeny (Swanson-Hysell et al., 2023). It is during this ca. 1010-980 Ma Rigolet phase of the orogeny that the Grenville Front developed (Rivers, 2008) which indicates that this was a time period when contractional deformation associated with the orogeny was propagating into the Superior craton. Together, the detrital zircon, sedimentology, and the fault calcite dates are consistent with the Jacobsville Formation being deposited in a syn-orogenic

573 Greenville backbulge basin and subsequently deformed as contraction associated with the
 574 Rigolet phase of the Grenville orogeny propagated into the interior of Laurentia.

575 Previously, some researchers have interpreted there to have been large-scale regional
 576 contractional deformation during the Alleghanian orogeny in the Paleozoic leading to
 577 reactivation of reverse faults including the Keweenaw Fault (Craddock et al., 2017). While
 578 the Keweenaw Fault is defined quite broadly in Craddock et al. (2017), the evidence put
 579 forward that is relevant to the segment in this study region are: 1) an interpreted post-
 580 Grenvillian orogeny age for the Jacobsville Formation which would require that the de-
 581 formation of the formation was associated with subsequent orogenesis; and 2) deforma-
 582 tion within two <1.5 km diameter outliers of Paleozoic sedimentary rocks that overlie
 583 the Jacobsville (Limestone Mountain in Figure 1). The data used to argue for a post-
 584 Grenvillian depositional age of the Jacobsville Formation were the low-precision LA-ICP-
 585 MS detrital zircon dates of Malone et al. (2016) that have now been superseded by the
 586 tandem dates of Hodgin et al. (2022). These dates are consistent with syn-Grenvillian
 587 deposition. This progress leaves the tilted and/or brecciated Paleozoic strata in the small
 588 exposed Paleozoic outliers of the 1.5 x 1 km Limestone Mountain and the neighboring
 589 0.5 x 0.3 km Sherman Hill as evidence of Paleozoic deformation: interpreted to be Pa-
 590 leozoic orogenesis by Hamblin (1958); Craddock et al. (2017) and suggested to be an im-
 591 pact structure by others (Milstein, 1987). The impact origin interpretation builds on pre-
 592 vious interpretations of the structure as being cryptovolcanic (Cannon & Mudrey, 1981)–
 593 a common interpretation for structures that have subsequently been recognized as im-
 594 pact related. The tilt and brecciation of these outliers contrasts with widespread flat-
 595 laying Paleozoic sedimentary rocks that overlie the reverse faults that underwent con-
 596 tractional deformation associated with rift inversion in Minnesota (Jirsa et al., 2011).
 597 These strata constrain Paleozoic deformation to have been relatively minor on the scale
 598 of 10s of meters rather than the kilometers of uplift associated with the rift inversion along
 599 these reverse faults (Boerboom et al., 2018). Clumped isotope temperatures of ~50°C
 600 from the Neoproterozoic fault calcite, also developed by Hodgin et al. (2022), reveal that
 601 the Keweenaw fault zone was within a couple kilometers of the surface at the time of late
 602 Mesoproterozoic to early Neoproterozoic calcite precipitation. These data are inconsis-
 603 tent with major Paleozoic uplift and support the interpretation that the majority of con-
 604 tractional inversion along the Keweenaw Fault occurred during the Rigolet Stage of the
 605 orogeny.

606 Our new paleomagnetic data provides additional insights into the timing of Jacob-
 607 sville deformation in the early Neoproterozoic. At the Snake Creek tributary section which
 608 is folded against the Keweenaw Fault (Figure 1, 2), the chemical remanence directions
 609 held by pigmentary hematite fail a fold test (Figure S4), indicating that the pigmentary
 610 hematite holding the remanence grew after deformation of the strata. The mean pole
 611 position of the chemical remanent magnetization at the Snake Creek tributary section
 612 overlaps with paleomagnetic poles of the Grenville Loop that have been assigned exhum-
 613 ation ages of ca. 970–960 Ma (Figure S7; Brown and McEnroe (2012)). This chemical re-
 614 manence pole position and the mean Jacobsville detrital remanence pole position are both
 615 far away from Laurentia’s pole positions at the times of Paleozoic orogenesis or any younger
 616 time in the Phanerozoic (Figure S7). This result indicates that the majority of the tilt-
 617 ing of the Jacobsville in the footwall of the Keweenaw Fault could not have occurred dur-
 618 ing Paleozoic orogenesis such as the Alleghanian orogeny as the chemical remanent mag-
 619 netization would then be expected to record a direction aligned with the Phanerozoic
 620 pole path. Instead, the Rigolet phase of Grenvillian orogeny, which ended by ca. 980 Ma,
 621 is the only feasible orogenic interval that could have tilted these strata. This result con-
 622 strains the Jacobsville Formation in the studied outcrop belt to have been deposited prior
 623 to ca. 980 Ma. While Paleozoic reactivation could have occurred, and there could be de-
 624 formation of that age elsewhere such as at Limestone Mountain, deformation at this time
 625 on the Keweenaw Fault would have been relatively minor compared to that in the early
 626 Neoproterozoic.

In conclusion, our paleomagnetic data and existing chronological data combined with the geological constraints are most consistent with the interpretation that the Jacobsville Formation within the studied bedrock belt was deposited in a syn-orogenic basin associated with the Rigolet Phase of the Grenvillian orogeny. This syn-orogenic basinal setting, which is consistent with the sedimentology of the formation (Fig. 2), provides a mechanism for developing accommodation space. The total duration of deposition of the Jacobsville is uncertain with these constraints alone particularly given the low precision on the 985.5 ± 35.8 Ma calcite date. However, data from the Grenville orogen itself constrain the end of the Rigolet phase to be ca. 980 Ma (Swanson-Hysell et al., 2023). As the studied sections proximal to the Keweenaw Fault were deformed in its footwall during this phase of contractional deformation, it is reasonable to interpret deposition as occurring before the ca. 980 Ma cessation of Grenvillian orogenesis. Taken together, we consider the best nominal age constraint for the depositional age of the Jacobsville Formation to pair with the Jacobsville paleomagnetic pole position to be ca. 990 Ma as the Rigolet phase of the orogeny was ongoing. While deposition within peripheral foreland basins typically lasts between 10 and 50 million years (Woodcock, 2004), the backbulge depocenter may not be as stable or long-lived. Given the available chronometric constraints from the Jacobsville Formation, the Keweenaw Fault and the Rigolet phase in the Grenville orogen, deposition of the Jacobsville can be considered to have occurred within the 1000 to 980 Ma time interval.

Slowdown of Laurentia's plate motion due to the Grenvillian orogeny

The ca. 1109-1070 Ma Keweenawan Track constrains rapid motion of Laurentia from high latitudes toward the equator (Fig. 9; Davis and Green (1997); Swanson-Hysell, Ramezani, et al. (2019)). Apparent polar wander path inversion results are consistent with the pole path being dominated by plate tectonic motion that could have reached a rate of 30 cm/yr (95% interval of 27-34 cm/yr; one Euler pole scenario; Swanson-Hysell, Ramezani, et al. (2019); Rose et al. (2022)); even faster than the rate of Indian plate motion during the closure of the Neotethys Ocean (van Hinsbergen, 2022; Jagoutz et al., 2015). Laurentia's rapid motion preceded and coincided with the onset of the collisional Grenvillian orogeny. In contrast to the rapid changes in pole position associated with the Keweenawan Track, the relatively close proximity between the ca. 990 Ma Jacobsville pole and ca. 1085 to 1070 Ma poles indicate that Laurentia's motion significantly slowed following the onset of the Grenvillian orogeny (Figs. 8 and 9). Lacking chronostratigraphic constraints, previous treatments have assigned an age to the Jacobsville pole of Roy and Robertson (1978) through extrapolation of the motion of the Keweenawan Track (e.g. Li et al., 2008). With the improved age constraints of Hodgin et al. (2022) and our new paleomagnetic pole, we can instead constrain that Laurentia's motion decreased by an order of magnitude. Incorporating temporal and spatial uncertainty on the poles gives APWP rate of ~ 3.2 cm/yr (95% interval from 2.5 cm/yr to 4.3 cm/yr; Fig. S8) between ca. 1070 to 990 Ma.

This slowdown in plate motion is geodynamically consistent with the onset of Grenvillian orogenesis. The earliest records of orogenesis on the leading margin of Laurentia occur ca. 1090 Ma with estimates of peak orogenesis associated with the Ottawan stage of the orogeny occurring ca. 1050 Ma (Rivers et al., 2012; Swanson-Hysell et al., 2023). Inversions of the Keweenawan Track that incorporate multiple tectonic Euler poles indicate a slowdown from rates exceeding 20 cm/yr prior to 1095 Ma to rates below 20 cm/yr after 1095 Ma (Swanson-Hysell, Ramezani, et al., 2019; Rose et al., 2022). This initial slowdown could be associated with soft collision as contractional deformation initiated on the leading edge of Laurentia (Staal & Zagorevski, 2020). Continued contractional collision led to substantially thickened crust recorded by granulite-facies metamorphic rocks by the time of peak Ottawan phase metamorphism ca. 1050 Ma (Rivers et al., 2012). The large slowdown in plate speed as now constrained by the Jacobsville paleomagnetic pole is associated with this progression to hard continent-continent collision involving

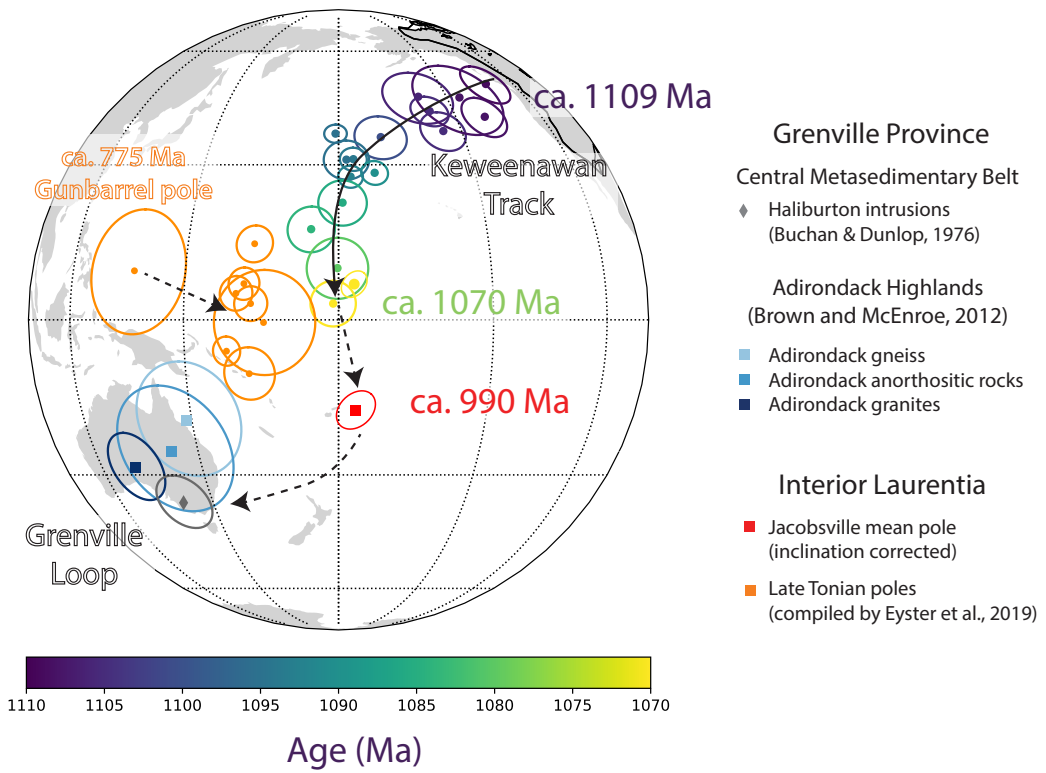


Figure 8. The inclination-corrected Jacobsdale Formation detrital remanent magnetization mean pole position with its Kent uncertainty ellipse is plotted in context of the ca. 1109–1070 Ma Keweenawan Track (poles color-coded by age shown in the colorbar), selected poles from the Grenville Province, and late Tonian poles of Laurentia as compiled by Eyster et al. (2019) (orange colored poles). The southerly pole position of the ca. 990 Ma Jacobsdale Formation indicates that the study area was crossing the equator in the late Mesoproterozoic to early Neoproterozoic. Given the large arc distance between the ca. 990 Ma Jacobsdale pole and the poles of the Grenville loop, such as those of the the Haliburton intrusions, we suggest that estimates of their age as >1000 Ma (Warnock et al., 2000; Halls, 2015; Evans, 2021) are likely too old. The solid curve with arrow represents a continuous path of the Keweenawan Track, the dashed curves with arrow represent inferred apparent polar wander in the early Neoproterozoic based on data developed and compiled in this study and by Eyster et al. (2019). The pole compilation used in this figure is included as Table S1.

increased crustal thickening and progressive transmission of contractional stress that eventually progressed into the interior of Laurentia (Cannon, 1994).

Laurentia's rapid motion was associated with closure of the Unimor Ocean and is consistent with it being on the lower plate that subducted under a conjugate continent (e.g. Amazonia) that collided on its margin (Swanson-Hysell et al. (2023); Fig. 9). The Jacobsdale paleomagnetic pole constrains this motion to have slowed as orogeny progressed to be a large-scale continent-continent collision. As a result, Laurentia maintained a low-latitude position throughout the duration of the Grenvillian orogeny which sutured continents together into the supercontinent Rodinia (Fig. 9).

689 **Implications for the age of the Grenville Loop**

690 Given that the age and pole position of the Jacobsville Formation had been un-
 691 certain and lacking other constraints from sedimentary or volcanic rocks, reconstruction
 692 of the paleogeography of Laurentia in the early Neoproterozoic has been reliant on pa-
 693 leomagnetic poles developed from metamorphic rocks within the Grenville Province (e.g.
 694 Weil et al., 1998). As is shown in Figure 8, paleomagnetic poles of the Grenville Loop
 695 plot near Australia in present-day coordinates; forming arc distances ranging from $\sim 35^\circ$
 696 to more than 50° away from poles at the end of the ca. 1110 to 1070 Ma Keweenawan
 697 Track (Fig. 8). Determining ages associated with the Grenville Loop poles is crucial for
 698 constraining the motion of Laurentia at this time and the configuration between Lau-
 699 rentia and hypothesized conjugate continents such as Baltica within Rodinia (Cawood
 700 & Pisarevsky, 2017; Gong et al., 2018; Swanson-Hysell, 2021).

701 In contrast to rocks of the Midcontinent Rift where magnetizations can be confi-
 702 dently assigned to be the same age as the crystallization ages of the rocks (e.g. Davis
 703 & Green, 1997; Fairchild et al., 2017; Swanson-Hysell, Ramezani, et al., 2019), rocks of
 704 the Grenville orogen experienced up to granulite facies metamorphism (temperatures $>900^\circ\text{C}$;
 705 e.g. Shinevar et al. (2021); Metzger et al. (2021)) and acquired magnetic remanence dur-
 706 ing subsequent exhumation (McWilliams & Dunlop, 1975; Dunlop & Stirling, 1985; Dod-
 707 son & McClelland-Brown, 1985). During slow post-orogenic exhumation ($1\text{-}3^\circ\text{C}/\text{Myr}$; e.g.
 708 Rivers and Volkert (2023)), magnetic minerals acquired remanence by cooling through
 709 an extended temperature range over millions to tens of millions of years (Pullaiah et al.,
 710 1975; Dodson & McClelland-Brown, 1980) or by crystallizing through exsolution (McEnroe
 711 et al., 2007). Determining the age of magnetization in such rocks requires reconstruct-
 712 ing cooling histories using isotopic thermochronometers which experience radioisotopic
 713 accumulation on mineral-specific closure of elemental diffusion (Dodson, 1973; Dodson
 714 & McClelland-Brown, 1985).

715 Based on the interpretation that blocking of magnetic remanence of the magnetite-
 716 bearing Haliburton intrusions of the Grenville Central Metamorphic Belt occurred dur-
 717 ing relatively narrow temperature ranges close to the Curie temperature of magnetite
 718 (i.e. 580°C), Warnock et al. (2000) considered that the timing of remanence acquisition
 719 during cooling of the intrusions is bracketed between U-Pb titanite and $^{40}\text{Ar}/^{39}\text{Ar}$ horn-
 720 blende dates. As a result, that study interpreted the age associated with the Halibur-
 721 ton paleomagnetic pole to be ca. 1015 Ma. This age has been assigned to the pole in sub-
 722 sequent compilations (e.g. Evans et al., 2021). In the central Adirondack Highlands of
 723 the Grenville orogen, magnetite-bearing granitic rocks and anorthositic rocks record pole
 724 positions that overlap with the Haliburton pole while their ages have been interpreted
 725 by Brown and McEnroe (2012) to be ca. 990-970 Ma, based on U-Pb and $^{40}\text{Ar}/^{39}\text{Ar}$ ther-
 726 mochronology data developed by Mezger et al. (1991). The ca. 990 Ma Jacobsville pole
 727 position is both distinct from the Grenville Loop poles and is consistent with a slowdown
 728 of Laurentia's plate motion associated with the Grenvillian orogeny (Fig. 8). If ages that
 729 have been assigned to Grenville Loop poles are taken at face value, those poles repre-
 730 sent the position of Laurentia both before and after the position constrained by the ca.
 731 990 Ma Jacobsville pole. Such an interpretation would imply either rapid plate tectonic
 732 motion of Laurentia coeval with the Rigolet phase of the Grenvillian orogeny or rapid
 733 oscillatory true polar wander (e.g. Evans, 2003). A more straightforward alternative model
 734 that could explain the distinct pole positions between the Jacobsville pole and the Grenville
 735 Loop poles is that the poles from the Grenville orogen are younger than currently inter-
 736 preted. Instead of having acquired remanence during the orogeny, the Grenville rocks
 737 could have acquired magnetic remanence during protracted exhumation that followed
 738 the ca. 980 Ma cessation of contractional deformation associated with the Rigolet stage
 739 of the orogeny. In this scenario, the migration of Rodinia to the higher latitude position
 740 represented by the Grenville loop poles would have occurred further into the Neoprotero-
 741 zoic after the Grenvillian orogeny had ceased.

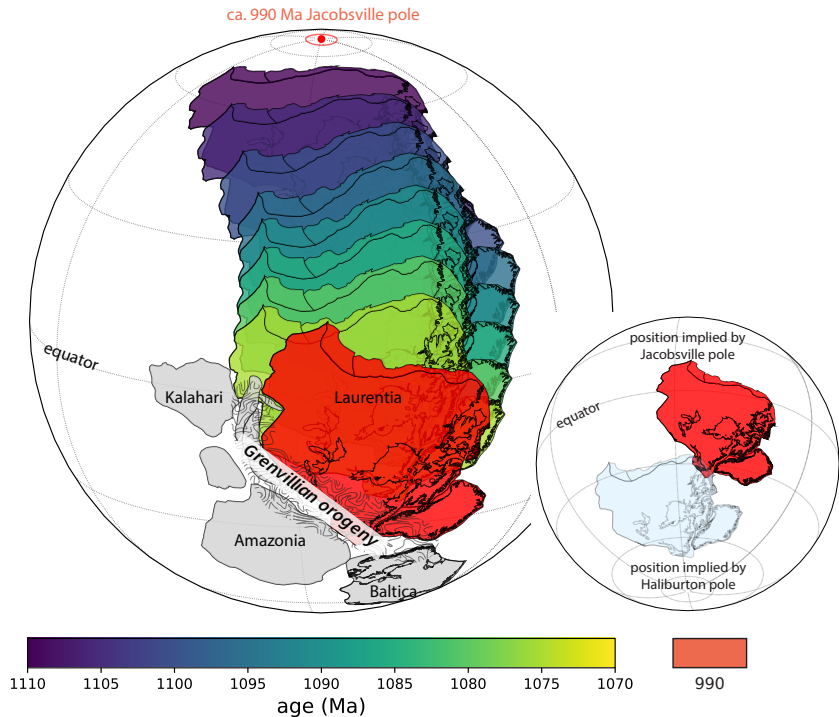


Figure 9. Paleogeographic position of Laurentia through the late Mesoproterozoic to early Neoproterozoic. The color-coded reconstructions show snapshots of Laurentia's position and orientation at 5 Myr intervals from 1110 to 1075 Ma. These reconstructions implement the two-stage tectonic Euler pole rotation inversion of Swanson-Hysell, Ramezani, et al. (2019). The paleogeographic snapshot colored in red shows the position and orientation of Laurentia ca. 990 Ma as constrained by the Jacobsville paleomagnetic pole developed in this study. Interpreted positions of Laurentia's conjugate continents along its margin are shown in grey. This reconstruction shows that while Laurentia experienced rapid latitudinal changes through the Keweenawan Track that its motion was much slower between ca. 1075 and 990 Ma as the Grenvillian orogeny progressed. The paleogeographic positions of conjugate continents to Laurentia long the Grenville margin in the reconstructions follow the interpretation of Swanson-Hysell et al. (2023). The inset figure compares Laurentia's position predicted by the new Jacobsville paleomagnetic pole (red) and that constrained by the Haliburton intrusions of the Grenvillian orogeny (light blue) which has been assigned an age of 1015 Ma (Warnock et al., 2000)). We suggest that this and other Grenville loop poles are younger and that Laurentia traveled from low latitudes toward higher latitudes following ca. 990 Ma while the Grenville orogen was slowly cooling and exhuming.

While numerous paleomagnetic data sets have been developed from rocks of the Grenville Province, few are paired with well-calibrated, high-precision thermochronology data. Recent data sets, such as new apatite U-Pb dates of 923 ± 14 Ma (2σ analytical uncertainty) from the Wilberforce pyroxenite (Paul et al., 2021), give tantalizing hints that temperatures that blocked magnetizations in portions of the orogen were achieved later than the ages assigned to paleomagnetic poles would suggest as U-Pb apatite closure temperatures are close to magnetite blocking temperatures (ca. 360-570°C; Cherniak et al. (1991)). To test the hypothesis that the Grenville Loop is younger than in previous interpretations, geochronology studies are needed to exploit the resolving power of high-precision whole grain analytical methods (i.e. ID-TIMS) and high-spatial-resolution

752 in-situ methods (e.g. laser ablation depth profiling; Chew and Spikings (2021)) for re-
 753 constructing the cooling rate and time-temperature history of the Grenville Province.
 754 Testing this hypothesis is critical for reconstructions of the paleogeography of Rodinia
 755 in the early Neoproterozoic.

756 Conclusion

757 The magnetization of hematite-bearing fine-grained siliciclastic sedimentary rocks
 758 from the Jacobsville Formation can be shown to be detrital and primary through pos-
 759 itive intraformational conglomerate and fold tests. We use these data to develop a new
 760 inclination-corrected paleomagnetic pole that can be constrained with recently published
 761 radiometric age constraints from Hodgin et al. (2022) to be ca. 990 Ma. This high-quality
 762 pole is a crucial addition to Laurentia's apparent polar wander path in the earliest Neo-
 763 proterozoic. Its position indicates that Laurentia's plate motion significantly slowed dur-
 764 ing Grenvillian collisional orogenesis. The new pole establishes a well-calibrated constraint
 765 for the position of the supercontinent Rodinia in early Neoproterozoic with Laurentia
 766 being at the center. The Jacobsville pole implies that ages associated with the paleo-
 767 magnetic poles recorded by metamorphic rocks of the Grenville Province are likely younger
 768 than in current interpretations. Further paired studies of high-quality paleomagnetism
 769 and high-precision thermochronology are needed to illuminate Rodinia's motion and con-
 770 figuration in the early Neoproterozoic.

771 Data Availability

772 Paleomagnetic data associated with this study are available within the MagIC database
 773 ([10.7288/V4/MAGIC/19780](https://doi.org/10.7288/V4/MAGIC/19780)) and all data are within a Github repository associated with
 774 this work (<https://github.com/Swanson-Hysell-Group/Jacobsville>) that is also archived
 775 on Zenodo (<https://zenodo.org/doi/10.5281/zenodo.10556464>; *will be archived in*
 776 *Zenodo upon acceptance*). This repository also contains Python code that implements
 777 all of the calculations, visualizations and statistical tests discussed herein.

778 Acknowledgments

779 Project research was funded by NSF CAREER grant EAR-1847277. Jim DeGraff pro-
 780 vided helpful guidance in identifying exposures of the Jacobsville Formation. We grate-
 781 fully acknowledge the Michigan Department of Natural Resources for sampling permit-
 782 ting. We thank Tim Lyons for additional private land access. We thank Madeline Swanson-
 783 Hysell for her assistance in the field. We thank David Malone, Douglas Elmore, and two
 784 anonymous reviewers for their helpful reviews.

785 References

- 786 Bilardello, D. (2016). The do's and don'ts of inclination shallowing corrections. *In-*
 787 *stitute for Rock Magnetism Quarterly*, 26(3), 1–9.
- 788 Bilardello, D., & Kodama, K. P. (2010). Palaeomagnetism and magnetic anisotropy
 789 of Carboniferous red beds from the Maritime Provinces of Canada: evidence
 790 for shallow palaeomagnetic inclinations and implications for North American
 791 apparent polar wander. *Geophysical Journal International*, 180(3), 1013–1029.
 792 doi: 10.1111/j.1365-246x.2009.04457.x
- 793 Boerboom, T., Bornhorst, T., Cannon, W., Hinze, W., Jirsa, M., Runkel, A.,
 794 ... Woodruff, L. (2018). Comment on “Paleozoic reactivation struc-
 795 tures in the Appalachian-Ouachita-Marathon foreland: Far-field defor-
 796 mation across Pangea, by J. Craddock, D. Malone, R. Porter, J. Com-
 797 ton, J. Luczaj, A. Konstantinou, J. Day, and S. Johnston [Earth Science
 798 Reviews 169 (2017), 1–34]. *Earth-Science Reviews*, 181, 144–152. doi:

- 799 10.1016/j.earscirev.2018.02.003
- 800 Books, K. G. (1968). Magnetization of the lowermost Keweenawan lava flows in
801 the Lake Superior area. *US Geological Survey Professional Paper*, 600, D248–
802 D254.
- 803 Books, K. G. (1972). Paleomagnetism of some Lake Superior Keweenawan rocks.
804 *Professional Paper*. doi: 10.3133/pp760
- 805 Brojanigo, A. (1984). *Keweenaw Fault: structures and sedimentology* (Unpublished
806 master's thesis). Michigan Technological University.
- 807 Brown, L., & McEnroe, S. (2012). Paleomagnetism and magnetic mineralogy of
808 Grenville metamorphic and igneous rocks, Adirondack Highlands, USA. , 212–
809 213, 57–74. doi: 10.1016/j.precamres.2012.04.012
- 810 Buchan, K. L., & Dunlop, D. J. (1976). Paleomagnetism of the Haliburton In-
811 trusions: Superimposed magnetizations, metamorphism, and tectonics in the
812 Late Precambrian. *Journal of Geophysical Research*, 81(17), 2951–2967. doi:
813 10.1029/jb081i017p02951
- 814 Bussy, F., Krogh, T. E., Klemens, W. P., & Schwerdtner, W. M. (1995). Tectonic
815 and metamorphic events in the westernmost Grenville Province, central On-
816 tario: new results from high-precision U–Pb zircon geochronology. *Canadian
817 Journal of Earth Sciences*, 32(5), 660–671. doi: 10.1139/e95-055
- 818 Cannon, W. F. (1989). The North American Midcontinent Rift beneath Lake Supe-
819 rior from GLIMPCE seismic reflection profiling. *Tectonics*, 8, 305–332.
- 820 Cannon, W. F. (1994). Closing of the Midcontinent Rift-A far-field effect of
821 Grenvillian compression. *Geology*, 22(2), 155. doi: 10.1130/0091-7613(1994)
822 022<0155:cotmra>2.3.co;2
- 823 Cannon, W. F., & Mudrey, M. G. (1981). *The potential for diamond-bearing kim-
824 berlite in northern Michigan and Wisconsin* (- ed.; Report). U.S. Geological
825 Surv. doi: 10.3133/cir842
- 826 Cannon, W. F., Nicholson, S., Woodruff, L., Hedgman, C., & Schulz, K. (1995).
827 Geologic map of the Ontonagon and part of the Wakefield 30'x60'quadrangles.
828 *Michigan: US Geological Survey Miscellaneous Investigations Series Map*,
829 1–2499.
- 830 Cannon, W. F., & Nicholson, S. W. (2001). Geologic map of the Keweenaw Penin-
831 sula and adjacent area, Michigan. *USGS Numbered Series*, 2696.
- 832 Cannon, W. F., Peterman, Z. E., & Sims, P. K. (1993). Crustal-scale thrusting and
833 origin of the Montreal River monocline-A 35-km-thick cross section of the mid-
834 continent rift in northern Michigan and Wisconsin. *Tectonics*, 12(3), 728–744.
835 doi: 10.1029/93tc00204
- 836 Cannon, W. F., Woodruff, L., Nicholson, S., & Hedgman, C. (1996). *Bedrock
837 geologic map of the Ashland and the northern part of the Ironwood 30- x 60-
838 minute quadrangles, Wisconsin and Michigan* (Tech. Rep.). U.S. Geological
839 Surv. doi: 10.3133/i2566
- 840 Cawood, P. A., & Pisarevsky, S. A. (2017). Laurentia-Baltica-Amazonia relations
841 during Rodinia assembly. *Precambrian Research*, 292, 386–397. doi: 10.1016/
842 j.precamres.2017.01.031
- 843 Cherniak, D., Lanford, W., & Ryerson, F. (1991). Lead diffusion in apatite
844 and zircon using ion implantation and Rutherford Backscattering tech-
845 niques. *Geochimica et Cosmochimica Acta*, 55(6), 1663–1673. doi:
846 10.1016/0016-7037(91)90137-t
- 847 Chew, D. M., & Spikings, R. A. (2021). Apatite U-Pb Thermochronology: A Re-
848 view. *Minerals*, 11(10), 1095. doi: 10.3390/min11101095
- 849 Collinson, D. W. (1965). Origin of remanent magnetization and initial susceptibility
850 of certain red sandstones. *Geophysical Journal International*, 9(2-3), 203–217.
851 doi: 10.1111/j.1365-246x.1965.tb02071.x
- 852 Collinson, D. W. (1974). The role of pigment and specularite in the remanent mag-
853 netism of red sandstones. *Geophysical Journal International*, 38(2), 253–264.

- doi: 10.1111/j.1365-246x.1974.tb04119.x
- Craddock, J. P., Konstantinou, A., Vervoort, J. D., Wirth, K. R., Davidson, C., Finley-Blasi, L., ... Walker, E. (2013). Detrital zircon provenance of the Mesoproterozoic Midcontinent Rift, Lake Superior region, U.S.A. *The Journal of Geology*, 121(1), 57–73. doi: 10.1086/668635
- Craddock, J. P., Malone, D. H., Porter, R., Compton, J., Luczaj, J., Konstantinou, A., ... Johnston, S. T. (2017). Paleozoic reactivation structures in the Appalachian-Ouachita-Marathon foreland: Far-field deformation across Pangea. *Earth-Science Reviews*, 169, 1–34. doi: 10.1016/j.earscirev.2017.04.002
- Daniels, P. A. (1982). 7C: Upper Precambrian sedimentary rocks: Oronto Group, Michigan-Wisconsin. In *Geological Society of America Memoirs* (pp. 107–134). Geological Society of America. doi: 10.1130/mem156-p107
- Davis, D. W., & Green, J. C. (1997). Geochronology of the North American Midcontinent Rift in western Lake Superior and implications for its geodynamic evolution. *Canadian Journal of Earth Sciences*, 34(4), 476–488. doi: 10.1139/e97-039
- Davis, D. W., & Sutcliffe, R. H. (1985). U-Pb ages from the Nipigon plate and northern Lake Superior. *Geological Society of America Bulletin*, 96(12), 1572. doi: 10.1130/0016-7606(1985)96<1572:uaftnp>2.0.co;2
- DeGraff, J. M., & Carter, B. T. (2022). Detached structural model of the Keweenaw fault system, Lake Superior region, North America: Implications for its origin and relationship to the Midcontinent Rift System. *GSA Bulletin*. doi: 10.1130/b36186.1
- Denyszyn, S. W., Halls, H. C., Davis, D. W., & Evans, D. A. (2009). Paleomagnetism and U-Pb geochronology of Franklin dykes in High Arctic Canada and Greenland: a revised age and paleomagnetic pole constraining block rotations in the Nares Strait region. *Canadian Journal of Earth Sciences*, 46(9), 689–705. doi: 10.1139/e09-042
- Diehl, J. F., & Haig, T. D. (1994). A paleomagnetic study of the lava flows within the Copper Harbor Conglomerate, Michigan: new results and implications. *Canadian Journal of Earth Sciences*, 31(2), 369–380. doi: 10.1139/e94-034
- Dodson, M. H. (1973). Closure temperature in cooling geochronological and petrological systems. *Contributions to Mineralogy and Petrology*, 40(3), 259–274. doi: 10.1007/bf00373790
- Dodson, M. H., & McClelland-Brown, E. (1980). Magnetic blocking temperatures of single-domain grains during slow cooling. *Journal of Geophysical Research*, 85(B5), 2625. doi: 10.1029/jb085ib05p02625
- Dodson, M. H., & McClelland-Brown, E. (1985). Isotopic and palaeomagnetic evidence for rates of cooling, uplift and erosion. *Geological Society, London, Memoirs*, 10(1), 315–325. doi: 10.1144/gsl.mem.1985.010.01.26
- Driscoll, P. E., & Evans, D. A. (2016). Frequency of Proterozoic geomagnetic superchrons. *Earth and Planetary Science Letters*, 437, 9–14. doi: 10.1016/j.epsl.2015.12.035
- Dubois, P. M. (1962). Palaeomagnetism and correlation of Keweenawan rocks. doi: 10.4095/100589
- Dunlop, D. J., & Stirling, J. M. (1985). Post-tectonic magnetizations from the Cordova gabbro, Ontario and Palaeozoic reactivation in the Grenville Province. *Geophysical Journal International*, 81(3), 521–550. doi: 10.1111/j.1365-246x.1985.tb06420.x
- Evans, D. A. D. (2003). True polar wander and supercontinents. *Tectonophysics*, 362(1-4), 303–320. doi: 10.1016/s0040-1951(02)000642-x
- Evans, D. A. D. (2021). Meso-Neoproterozoic Rodinia supercycle. In *Ancient Supercontinents and the Paleogeography of Earth* (pp. 549–576). Elsevier. doi: 10.1016/b978-0-12-818533-9.00006-0

- Evans, D. A. D., Pesonen, L. J., Eglington, B. M., Elming, S.-Å., Gong, Z., Li, Z.-X., ... Zhang, S. (2021). An expanding list of reliable paleomagnetic poles for Precambrian tectonic reconstructions. In (pp. 605–639). Elsevier. doi: 10.1016/b978-0-12-818533-9.00007-2
- Eyster, A., Weiss, B. P., Karlstrom, K., & Macdonald, F. A. (2019). Paleomagnetism of the Chuar Group and evaluation of the late Tonian Laurentian apparent polar wander path with implications for the makeup and breakup of Rodinia. *GSA Bulletin*. doi: 10.1130/b32012.1
- Fairchild, L. M., Swanson-Hysell, N. L., Ramezani, J., Sprain, C. J., & Bowring, S. A. (2017). The end of Midcontinent Rift magmatism and the paleogeography of Laurentia. *Lithosphere*, 9(1), 117–133. doi: 10.1130/l1580.1
- Fisher, R. (1953). Dispersion on a sphere. *Proceedings of the Royal Society A: Mathematical, Physical and Engineering Sciences*, 217(1130), 295–305. doi: 10.1098/rspa.1953.0064
- Gong, Z., Evans, D. A., Elming, S.-Å., Söderlund, U., & Salminen, J. M. (2018). Paleomagnetism, magnetic anisotropy and U-Pb baddeleyite geochronology of the early Neoproterozoic Blekinge-Dalarna dolerite dykes, Sweden. *Precambrian Research*, 317, 14–32. doi: 10.1016/j.precamres.2018.08.019
- Greenman, J. W., Rooney, A. D., Patzke, M., Ielpi, A., & Halverson, G. P. (2021). Re-Os geochronology highlights widespread latest Mesoproterozoic (ca. 1090–1050 Ma) cratonic basin development on northern Laurentia. *Geology*. doi: 10.1130/g48521.1
- Haddox, C. A., & Dott, R. H. (1990). Cambrian shoreline deposits in northern Michigan. *Journal of Sedimentary Research*, 60(5), 697–716. doi: 10.1306/212F9250-2B24-11D7-8648000102C1865D
- Halls, H. C. (1974). A paleomagnetic reversal in the Osler Volcanic Group, northern Lake Superior. *Canadian Journal of Earth Sciences*, 11(9), 1200–1207. doi: 10.1139/e74-113
- Halls, H. C. (2015). Paleomagnetic evidence for ~4000 km of crustal shortening across the 1 Ga Grenville orogen of North America. *Geology*, G37188.1. doi: 10.1130/g37188.1
- Halls, H. C., & Pesonen, L. J. (1982). 9: Paleomagnetism of Keweenawan rocks. *Geology and Tectonics of the Lake Superior Basin*, 173–202. doi: 10.1130/mem156-p173
- Hamblin, W. K. (1958). Cambrian sandstones of northern Michigan. *Michigan Geological Survey Publication*.
- Harlan, S. S., Heaman, L., LeCheminant, A. N., & Premo, W. R. (2003). Gun-barrel mafic magmatic event: A key 780 Ma time marker for Rodinia plate reconstructions. *Geology*, 31(12), 1053. doi: 10.1130/g19944.1
- Hedgman, C. (1992). *Provenance and tectonic setting of the Jacobsville Sandstone, from Ironwood to Keweenaw Bay, Michigan* (Unpublished master's thesis). University of Cincinnati. Department of Geology.
- Henry, S. G., Mauk, F. J., & der Voo, R. V. (1977). Paleomagnetism of the upper Keweenawan sediments: the Nonesuch Shale and Freda Sandstone. *Canadian Journal of Earth Sciences*, 14(5), 1128–1138. doi: 10.1139/e77-103
- Hnat, J. S., van der Pluijm, B. A., & van der Voo, R. (2006). Primary curvature in the Mid-Continent Rift: Paleomagnetism of the Portage Lake Volcanics (northern Michigan, USA). *Tectonophysics*, 425(1-4), 71–82. doi: 10.1016/j.tecto.2006.07.006
- Hodgin, E. B., Swanson-Hysell, N. L., DeGraff, J. M., Kylander-Clark, A. R., Schmitz, M. D., Turner, A. C., ... Stolper, D. A. (2022). Final inversion of the Midcontinent Rift during the Rigolet Phase of the Grenvillian Orogeny. *Geology*. doi: 10.1130/g49439.1
- Irving, R. D., & Chamberlin, T. C. (1885). *Observations on the junction between the Eastern sandstone and the Keweenaw series on Keweenaw Point, Lake*

- 964 *Superior* (Tech. Rep.). U.S. Geological Survey. doi: 10.3133/b23
- 965 Jagoutz, O., Royden, L., Holt, A. F., & Becker, T. W. (2015). Anomalously fast
966 convergence of India and Eurasia caused by double subduction. *Nature Geosci-
967 ence*, 8(6), 475–478. doi: 10.1038/ngeo2418
- 968 Jannin, S., Gervais, F., Moukhsil, A., & Augland, L. E. (2018). Late-Grenvillian
969 channel flow in the central Grenville Province (Manicouagan Reservoir area):
970 New constraints from a structural and geochronological study of the Al-
971 lochthon Boundary Thrust. *Journal of Structural Geology*, 115, 132–151.
972 doi: 10.1016/j.jsg.2018.07.019
- 973 Jiang, Z., Liu, Q., Dekkers, M. J., Tauxe, L., Qin, H., Barrón, V., & Torrent, J.
974 (2015). Acquisition of chemical remanent magnetization during experimental
975 ferrihydrite–hematite conversion in Earth-like magnetic field—implications for
976 paleomagnetic studies of red beds. *Earth and Planetary Science Letters*, 428,
977 1–10. doi: 10.1016/j.epsl.2015.07.024
- 978 Jiang, Z., Liu, Q., Roberts, A. P., Barrón, V., Torrent, J., & Zhang, Q. (2018). A
979 new model for transformation of ferrihydrite to hematite in soils and sedi-
980 ments. *Geology*. doi: 10.1130/g45386.1
- 981 Jirsa, M. A., Boerboom, T., Chandler, V., Mossler, J., Runkel, A., & Setterholm,
982 D. (2011). *S-21 Geologic map of Minnesota-bedrock geology* (Tech. Rep.).
983 Minnesota Geological Survey.
- 984 Kalliokoski, J. (1982). 7E: Jacobsville Sandstone. *Geology and Tectonics of the Lake
985 Superior Basin*, 147–156. doi: 10.1130/mem156-p147
- 986 Karlstrom, K., Mohr, M., Schmitz, M., Sundberg, F., Rowland, S., Blakey, R.,
987 ... Hagadorn, J. (2020). Redefining the Tonto Group of Grand Canyon
988 and recalibrating the Cambrian time scale. *Geology*, 48(5), 425–430. doi:
989 10.1130/g46755.1
- 990 Kent, J. T. (1982). The Fisher-Bingham distribution on the sphere. *Journal of
991 the Royal Statistical Society: Series B (Methodological)*, 44(1), 71–80. doi: 10
992 .1111/j.2517-6161.1982.tb01189.x
- 993 King, R. F. (1955). The remanent magnetism of artificially deposited sediments.
994 *Geophysical Journal International*, 7, 115–134. doi: 10.1111/j.1365-246x.1955
995 .tb06558.x
- 996 Kirschvink, J. L. (1980). The least-squares line and plane and the analysis of palaeo-
997 magnetic data. *Geophysical Journal International*, 62(3), 699–718. doi: 10
998 .1111/j.1365-246x.1980.tb02601.x
- 999 Li, Z., Bogdanova, S., Collins, A., Davidson, A., Waele, B. D., Ernst, R., ...
1000 Vernikovsky, V. (2008). Assembly, configuration, and break-up history
1001 of Rodinia: A synthesis. *Precambrian Research*, 160(1-2), 179–210. doi:
1002 10.1016/j.precamres.2007.04.021
- 1003 Macdonald, F. A., Yonkee, W. A., Flowers, R. M., & Swanson-Hysell, N. L. (2023).
1004 Neoproterozoic of Laurentia. In *Laurentia: Turning points in the evolution of
1005 a continent* (pp. 331–380). Geological Society of America. doi: 10.1130/2022
1006 .1220(19)
- 1007 Mackinder, A., Cousens, B. L., Ernst, R. E., & Chamberlain, K. R. (2019). Geo-
1008 chemical, isotopic, and U–Pb zircon study of the central and southern portions
1009 of the 780 Ma Gunbarrel Large Igneous Province in western Laurentia. *Can-
1010 adian Journal of Earth Sciences*, 56(7), 738–755. doi: 10.1139/cjes-2018-0083
- 1011 Malone, D. H., Stein, C. A., Craddock, J. P., Kley, J., Stein, S., & Malone, J. E.
1012 (2016). Maximum depositional age of the Neoproterozoic Jacobsville Sand-
1013 stone, Michigan: Implications for the evolution of the Midcontinent Rift.
1014 *Geosphere*, 12(4), 1271–1282. doi: 10.1130/ges01302.1
- 1015 Malone, D. H., Stein, C. A., Craddock, J. P., Stein, S., & Malone, J. E. (2020).
1016 Neoproterozoic sedimentation and tectonics of the Laurentian midcontinent:
1017 Detrital zircon provenance of the Jacobsville Sandstone, Lake Superior Basin,
1018 USA and Canada. *Terra Nova*. doi: 10.1111/ter.12481

- 1019 Manson, M. L., & Halls, H. C. (1994). Post-Keweenawan compressional faults in the
 1020 eastern Lake Superior region and their tectonic significance. *Canadian Journal*
 1021 *of Earth Sciences*, 31(4), 640–651. doi: 10.1139/e94-057
- 1022 McCabe, C., & Van der Voo, R. (1983). Paleomagnetic results from the upper Ke-
 1023 weenawan Chequamegon Sandstone: implications for red bed diagenesis and
 1024 Late Precambrian apparent polar wander of North America. *Canadian Journal*
 1025 *of Earth Sciences*, 20(1), 105–112. doi: 10.1139/e83-010
- 1026 McEnroe, S. A., Robinson, P., Langenhorst, F., Frandsen, C., Terry, M. P., & Bal-
 1027 laran, T. B. (2007). Magnetization of exsolution intergrowths of hematite and
 1028 ilmenite: Mineral chemistry, phase relations, and magnetic properties of hemo-
 1029 ilmenite ores with micron- to nanometer-scale lamellae from Allard Lake, Que-
 1030 bec. *Journal of Geophysical Research*, 112(B10). doi: 10.1029/2007jb004973
- 1031 McFadden, P., & McElhinny, M. (1990). Classification of the reversal test in palaeo-
 1032 magnetism. *Geophysical Journal International*, 103, 725–729. doi: 10.1111/j.
 1033 .1365-246X.1990.tb05683.x
- 1034 McWilliams, M. O., & Dunlop, D. J. (1975). Precambrian paleomagnetism: magne-
 1035 tizations reset by the Grenville Orogeny. *Science*, 190(4211), 269–272. doi: 10
 1036 .1126/science.190.4211.269
- 1037 Metzger, E. P., Leech, M. L., Davis, M. W., Reeder, J. V., Swanson, B. A., & War-
 1038 ing, H. V. (2021). Ultrahigh-temperature granulite-facies metamorphism and
 1039 exhumation of deep crust in a migmatite dome during late- to post- orogenic
 1040 collapse and extension in the central Adirondack Highlands (New York, USA).
 1041 *Geosphere*. doi: 10.1130/ges02318.1
- 1042 Mezger, K., Rawnsley, C. M., Bohlen, S. R., & Hanson, G. N. (1991). U-Pb garnet,
 1043 sphene, monazite, and rutile ages: Implications for the duration of high-grade
 1044 metamorphism and cooling histories, Adirondack Mts., New York. , 99(3),
 1045 415–428. doi: 10.1086/629503
- 1046 Milstein, R. L. (1987). Anomalous Paleozoic outliers near Limestone Mountain,
 1047 Michigan. In *North-Central Section of the Geological Society of America* (pp.
 1048 263–268). Geological Society of America. doi: 10.1130/0-8137-5403-8.263
- 1049 Mueller, S. A. (2021). *Structural analysis and interpretation of deformation*
 1050 *along the Keweenaw fault system west of Lake Gratiot, Keweenaw County,*
 1051 *Michigan* (Master's thesis, Michigan Technological University). doi:
 1052 10.37099/mtu.dc.etdr/1167
- 1053 Nabavi, S. T., & Fossen, H. (2021). Fold geometry and folding – a review. *Earth-*
 1054 *Science Reviews*, 222, 103812. doi: 10.1016/j.earscirev.2021.103812
- 1055 Nicholson, S. W., Dicken, C. L., Foose, M. P., & Mueller, J. (2004). *Integrated*
 1056 *geologic map databases for the United States; the upper midwest states: Min-*
 1057 *nesota, Wisconsin, Michigan, Illinois, and Indiana* (Tech. Rep.). US Geologi-
 1058 *cal Survey*.
- 1059 Ojakangas, R. W., & Dickas, A. B. (2002). The 1.1-Ga Midcontinent Rift Sys-
 1060 tem, central North America: sedimentology of two deep boreholes, Lake
 1061 Superior region. *Sedimentary Geology*, 147(1-2), 13–36. doi: 10.1016/
 1062 s0037-0738(01)00185-3
- 1063 Ojakangas, R. W., Morey, G., & Green, J. (2001). The Mesoproterozoic Midconti-
 1064 nent Rift System, Lake Superior Region, USA. *Sedimentary Geology*, 141-142,
 1065 421–442. doi: 10.1016/s0037-0738(01)00085-9
- 1066 Palmer, H. C., & Halls, H. C. (1986). Paleomagnetism of the Powder Mill Group,
 1067 Michigan and Wisconsin: A reassessment of the Logan Loop. *Journal of Geo-*
 1068 *physical Research*, 91(B11), 11571. doi: 10.1029/jb091ib11p11571
- 1069 Paul, A. N., Spikings, R. A., & Gaynor, S. P. (2021). U-Pb ID-TIMS reference
 1070 ages and initial Pb isotope compositions for Durango and Wilberforce apatites.
 1071 *Chemical Geology*, 586, 120604. doi: 10.1016/j.chemgeo.2021.120604
- 1072 Pierce, J., Zhang, Y., Hodgin, E. B., & Swanson-Hysell, N. L. (2022). Quantifying
 1073 inclination shallowing and representing flattening uncertainty in sedimentary

- 1074 paleomagnetic poles. *Geochemistry, Geophysics, Geosystems*, 23(11). doi:
 1075 10.1029/2022gc010682
- 1076 Pueyo, E., s, J. P., n, H. M., & 1, A. P. (2003). Conical folds and apparent rotations
 1077 in paleomagnetism (a case study in the Southern Pyrenees). *Tectonophysics*,
 1078 362(1-4), 345–366. doi: 10.1016/s0040-1951(02)00645-5
- 1079 Pullaiah, G., Irving, E., Buchan, K., & Dunlop, D. (1975). Magnetization changes
 1080 caused by burial and uplift. *Earth and Planetary Science Letters*, 28(2), 133–
 1081 143. doi: 10.1016/0012-821x(75)90221-6
- 1082 Rivers, T. (2008). Assembly and preservation of lower, mid, and upper orogenic
 1083 crust in the Grenville Province—Implications for the evolution of large hot
 1084 long-duration orogens. *Precambrian Research*, 167(3-4), 237–259. doi:
 1085 10.1016/j.precamres.2008.08.005
- 1086 Rivers, T., Culshaw, N., Hynes, A., Indares, A., Jamieson, R., Martignole, J., ...
 1087 Clowes, R. (2012). The Grenville Orogen—a post-LITHOPROBE perspective.
 1088 *tectonic styles in Canada: The lithoprobe perspective*, 49, 97–236.
- 1089 Rivers, T., & Volkert, R. A. (2023). Slow cooling in the metamorphic cores of
 1090 Grenvillian large metamorphic core complexes and the thermal signature of
 1091 the Ottawan orogenic lid. In *Laurentia: Turning points in the evolution of a*
 1092 *continent*. Geological Society of America. doi: 10.1130/2022.1220(16)
- 1093 Rose, I. R., Zhang, Y., & Swanson-Hysell, N. L. (2022). Bayesian paleomagnetic Eu-
 1094 ler pole inversion for paleogeographic reconstruction and analysis. *Journal of*
 1095 *Geophysical Research: Solid Earth*. doi: 10.1029/2021jb023890
- 1096 Roy, J. L., & Robertson, W. A. (1978). Paleomagnetism of the Jacobsville
 1097 Formation and the apparent polar path for the interval -1100 to -670 m.y.
 1098 for North America. *Journal of Geophysical Research*, 83(B3), 1289. doi:
 1099 10.1029/jb083ib03p01289
- 1100 Sapienza, F., Gallo, L. C., Zhang, Y., Vaes, B., Domeier, M., & Swanson-Hysell,
 1101 N. L. (2023). Quantitative analysis of paleomagnetic sampling strategies.
 1102 doi: 10.22541/essoar.168881772.25833701/v1
- 1103 Shinevar, W. J., Jagoutz, O., & VanTongeren, J. A. (2021). Gore Mountain gar-
 1104 net amphibolite records UHT conditions: implications for the rheology of the
 1105 lower continental crust during orogenesis. *Journal of Petrology*, 62(4). doi:
 1106 10.1093/petrology/egab007
- 1107 Slotznick, S. P., Swanson-Hysell, N. L., Zhang, Y., Clayton, K. E., Wellman, C. H.,
 1108 Tosca, N. J., & Strother, P. K. (2023). Reconstructing the paleoenviron-
 1109 ment of an oxygenated Mesoproterozoic shoreline and its record of life. *GSA*
 1110 *Bulletin*. doi: 10.1130/B36634.1
- 1111 Staal, C. V., & Zagorevski, A. (2020). Accretion, soft and hard collision: similarities,
 1112 differences and an application from the Newfoundland Appalachian orogen.
 1113 *Geoscience Canada*, 47(3), 103–118. doi: 10.12789/geocanj.2020.47.161
- 1114 Steiner, M. B. (1983). Detrital remanent magnetization in hematite. *Journal of Geo-*
 1115 *physical Research*, 88(B8), 6523. doi: 10.1029/jb088ib08p06523
- 1116 Swanson-Hysell, N. L. (2021). The Precambrian paleogeography of Laurentia. In *An-*
 1117 *cient Supercontinents and the Paleogeography of Earth* (pp. 109–153). Elsevier.
 1118 doi: 10.1016/b978-0-12-818533-9.00009-6
- 1119 Swanson-Hysell, N. L., Burgess, S. D., Maloof, A. C., & Bowring, S. A. (2014). Mag-
 1120 matic activity and plate motion during the latent stage of Midcontinent Rift
 1121 development. *Geology*, 42(6), 475–478. doi: 10.1130/g35271.1
- 1122 Swanson-Hysell, N. L., Fairchild, L. M., & Slotznick, S. P. (2019). Primary
 1123 and secondary red bed magnetization constrained by fluvial intraclasts.
 1124 *Journal of Geophysical Research: Solid Earth*, 124(5), 4276–4289. doi:
 1125 10.1029/2018jb017067
- 1126 Swanson-Hysell, N. L., Ramezani, J., Fairchild, L. M., & Rose, I. R. (2019). Failed
 1127 rifting and fast drifting: Midcontinent Rift development, Laurentia's rapid mo-
 1128 tion and the driver of Grenvillian orogenesis. *GSA Bulletin*, 131(5-6), 913–940.

- 1129 doi: 10.1130/b31944.1
- 1130 Swanson-Hysell, N. L., Rivers, T., & van der Lee, S. (2023). The late Mesoproterozoic to early Neoproterozoic Grenvillian orogeny and the assembly of Rodinia: Turning point in the tectonic evolution of Laurentia. In *Laurentia: Turning points in the evolution of a continent*. Geological Society of America. doi: 10.1130/2022.1220(14)
- 1135 Swanson-Hysell, N. L., Vaughan, A. A., Mustain, M. R., & Asp, K. E. (2014). Confirmation of progressive plate motion during the Midcontinent Rift's early magmatic stage from the Osler Volcanic Group, Ontario, Canada. *Geochemistry, Geophysics, Geosystems*, 15(5), 2039–2047. doi: 10.1002/2013gc005180
- 1139 Tauxe, L., & Kent, D. V. (1984). Properties of a detrital remanence carried by haematite from study of modern river deposits and laboratory redeposition experiments. *Geophysical Journal International*, 76(3), 543–561. doi: 10.1111/j.1365-246x.1984.tb01909.x
- 1143 Tauxe, L., & Kent, D. V. (2004). A simplified statistical model for the geomagnetic field and the detection of shallow bias in paleomagnetic inclinations: was the ancient magnetic field dipolar? *Geophysical Monograph Series*, 101–115. doi: 10.1029/145gm08
- 1147 Tauxe, L., Kent, D. V., & Opdyke, N. D. (1980). Magnetic components contributing to the NRM of Middle Siwalik red beds. *Earth and Planetary Science Letters*, 47(2), 279–284. doi: 10.1016/0012-821x(80)90044-8
- 1150 Tauxe, L., & Kodama, K. P. (2009). Paleosecular variation models for ancient times: Clues from Keweenawan lava flows. *Physics of the Earth and Planetary Interiors*, 177(1-2), 31–45. doi: 10.1016/j.pepi.2009.07.006
- 1153 Tauxe, L., Kylstra, N., & Constable, C. (1991). Bootstrap statistics for paleomagnetic data. *Journal of Geophysical Research*, 96(B7), 11723. doi: 10.1029/91jb00572
- 1156 Tauxe, L., Shaar, R., Jonestrask, L., Swanson-Hysell, N. L., Minnett, R., Koppers, A. A. P., ... Fairchild, L. (2016). PmagPy: Software package for paleomagnetic data analysis and a bridge to the Magnetics Information Consortium (MagIC) Database. *Geochemistry, Geophysics, Geosystems*, 17(6), 2450–2463. doi: 10.1002/2016gc006307
- 1161 Tauxe, L., & Watson, G. (1994). The fold test: an eigen analysis approach. *Earth and Planetary Science Letters*, 122(3-4), 331–341. doi: 10.1016/0012-821x(94)90006-x
- 1164 Thwaites, F. T. (1912). *Sandstones of the Wisconsin coast of Lake Superior* (Vol. 8). Wisconsin Geological and Natural History Survey.
- 1166 Torsvik, T. H., Van der Voo, R., Preeden, U., Mac Niocaill, C., Steinberger, B., Doubrovine, P. V., ... et al. (2012). Phanerozoic polar wander, palaeogeography and dynamics. *Earth-Science Reviews*, 114(3-4), 325–368. doi: 10.1016/j.earscirev.2012.06.007
- 1170 Turlin, F., Vanderhaeghe, O., Gervais, F., André-Mayer, A.-S., Moukhsil, A., Zeh, A., ... I.P.T.N. (2019). Petrogenesis of LREE-rich pegmatitic granite dykes in the central Grenville Province by partial melting of Paleoproterozoic-Archean metasedimentary rocks: Evidence from zircon U-Pb-Hf-O isotope and trace element analyses. *Precambrian Research*, 327, 327–360. doi: 10.1016/j.precamres.2019.02.009
- 1176 Tyrrell, C. (2019). *Keweenaw fault geometry and slip kinematics-Bête Grise Bay, Keweenaw Peninsula, Michigan* (Master's thesis, Michigan Technological University). doi: 10.37099/mtu.dc.edtr/947
- 1179 Vaes, B., Li, S., Langereis, C. G., & van Hinsbergen, D. J. J. (2021). Reliability of palaeomagnetic poles from sedimentary rocks. *Geophysical Journal International*, 225(2), 1281–1303. doi: 10.1093/gji/ggab016
- 1182 van Hinsbergen, D. J. J. (2022). Indian plate paleogeography, subduction and horizontal underthrusting below Tibet: paradoxes, controversies and opportunities.
- 1183

- 1184 *National Science Review*, 9(8). doi: 10.1093/nsr/nwac074
- 1185 Wallace, D. M. I. (1971). *The sedimentology and tectonic significance of the Bay-*
 1186 *field Group (Upper Keweenawan?), Wisconsin and Minnesota* (Unpublished
 1187 doctoral dissertation). The University of Wisconsin-Madison.
- 1188 Warnock, A. C., Kodama, K. P., & Zeitler, P. K. (2000). Using thermochronom-
 1189 etry and low-temperature demagnetization to accurately date Precambrian
 1190 paleomagnetic poles. *Journal of Geophysical Research: Solid Earth*, 105(B8),
 1191 19435–19453. doi: 10.1029/2000jb900114
- 1192 Watson, G. S. (1956). A test for randomness of directions. *Geophysical Journal In-*
 1193 *ternational*, 7, 160–161. doi: 10.1111/j.1365-246x.1956.tb05561.x
- 1194 Weil, A. B., der Voo, R. V., Niocaill, C. M., & Meert, J. G. (1998). The Protero-
 1195 zoic supercontinent Rodinia: paleomagnetically derived reconstructions for
 1196 1100 to 800 Ma. *Earth and Planetary Science Letters*, 154(1-4), 13–24. doi:
 1197 10.1016/s0012-821x(97)00127-1
- 1198 Weil, A. B., Geissman, J. W., & Ashby, J. M. (2006). A new paleomagnetic
 1199 pole for the Neoproterozoic Uinta Mountain supergroup, Central Rocky
 1200 Mountain States, USA. *Precambrian Research*, 147(3-4), 234–259. doi:
 1201 10.1016/j.precamres.2006.01.017
- 1202 Weil, A. B., Geissman, J. W., Heizler, M., & Van der Voo, R. (2003). Paleomag-
 1203 netism of Middle Proterozoic mafic intrusions and Upper Proterozoic
 1204 (Nankoweap) red beds from the Lower Grand Canyon Supergroup, Arizona.
 1205 *Tectonophysics*, 375(1-4), 199–220. doi: 10.1016/s0040-1951(03)00339-1
- 1206 Woodcock, N. H. (2004). Life span and fate of basins. *Geology*, 32(8), 685. doi: 10
 1207 .1130/g20598.1
- 1208 Zbinden, E., Holland, H., Feakes, C., & Dobos, S. (1988). The Sturgeon Falls paleo-
 1209 sol and the composition of the atmosphere 1.1 Ga BP. *Precambrian Research*,
 1210 42(1-2), 141–163. doi: 10.1016/0301-9268(88)90014-9
- 1211 Zhang, Y., Hodgin, E. B., Alemu, T., Pierce, J., Fuentes, A., & Swanson-Hysell,
 1212 N. L. (2023a). *Tracking Rodinia into the Neoproterozoic: new paleomag-*
 1213 *netic constraints from the Jacobsville Formation [Dataset]*. Retrieved from
 1214 <https://doi.org/10.7288/V4/MAGIC/19780>
- 1215 Zhang, Y., Hodgin, E. B., Alemu, T., Pierce, J., Fuentes, A., & Swanson-Hysell,
 1216 N. L. (2023b). *Tracking Rodinia into the Neoproterozoic: new paleomag-*
 1217 *netic constraints from the Jacobsville Formation [Dataset]*. Retrieved from
 1218 <https://doi.org/XXX>
- 1219 Zhang, Y., Hodgin, E. B., Alemu, T., Pierce, J., Fuentes, A., & Swanson-Hysell,
 1220 N. L. (2023c). *Tracking Rodinia into the Neoproterozoic: new paleomag-*
 1221 *netic constraints from the Jacobsville Formation [Software]*. Retrieved from
 1222 <https://github.com/Swanson-Hysell-Group/Jacobsville>